공학석사 학위논문

Evaluation of Deformation Characteristics of Residual Soil using Borehole Pressure-Shear Test Apparatus

공내 재하-전단시험기를 이용한 풍화토의 변형 특성 평가

2021년 2월

서울대학교 대학원

건설환경공학부

김 재 규

Evaluation of Deformation Characteristics of Residual Soil using Borehole Pressure-Shear Test Apparatus

지도 교수 정 충 기

이 논문을 공학석사 학위논문으로 제출함

2020 년 12월

서울대학교 대학원
건설환경공학부
김 재 규

김재규의 공학석사 학위논문을 인준함
2021 년 2월

위 원 장 김 성 렬 (인)

부위원장 정 충 기 (인)

위 원 박 준 범 (인)

Abstract

Evaluation of Deformation Characteristics of Residual Soil using Borehole Pressure-Shear Test Apparatus

Kim, Jae-Gyu
Department of Civil & Environmental Engineering
The Graduate School
Seoul National University

The weathered zone (weathered soil and weathered rock) is used as the main foundation layer of various structures due to their high bearing capacity. Accordingly, evaluating the ground characteristics of the weathered zone is very important for securing the performance and stability of the structure during design. However, since it is hard to obtain undisturbed weathered soil samples and weathered rock cores for evaluation of ground properties, performing laboratory tests is difficult and the reliability of the results is low. Therefore, it is common to evaluate the ground characteristics of the weathered zone through field tests such as standard penetration test (SPT), pressuremeter test (PMT), and borehole shear test (BST).

The evaluation of the design parameters via the SPT uses the SPT-N value and the correlation equation between several parameters. However, An empirical correlation for sand is inappropriate for the weathered zone because

the SPT is limited to hard soil and not properly applicable to highly weathered rock.

Also, the PMT can evaluate the ground properties of the weathered zone, but there is a limitation that it cannot evaluate the strength properties of the ground, which are the cohesion and the internal friction angle. Lastly, the BST can evaluate the strength properties of the ground, but it is not suitable for testing the weathered zone as the BST apparatus is developed for sand.

In this thesis, the borehole pressure-shear test apparatus was developed to overcome the limitations of the existing PMT and BST. The developed testing device is suitable for the weathered zone by improving the loading systems and securing the capacity by the motor. Also, the test apparatus is capable of real-time automatic control and measurement. The developed test apparatus can evaluate both deformation characteristics and strength characteristics of the weathered zone. However, the vertical loading system of the developed test apparatus for strength evaluation is currently being studied and improved.

A triaxial compression test and a physical model test by developed apparatus were performed to verify the horizontal loading performance and validity of the evaluation on deformation characteristics of the test apparatus.

As a result of the physical model test by the developed test apparatus, the pressure-strain behavior of the ground according to the experimental conditions was properly assessed. Via this, verification of the horizontal loading performance using developed test apparatus.

Also, the validity of the evaluation of deformation modulus using the developed test apparatus was confirmed. Since the deformation modulus obtained from the physical model test and triaxial compression test showed similar results.

With the borehole pressure-shear test apparatus, it is expected to be able to evaluate the ground properties more quickly and efficiently when applied in the field.

Keywords: Residual soils, Borehole pressure-shear test apparatus, Pressuremeter test, Physical modeling, Calibration chamber, Deformation characteristics

Student Number: 2018-27331

CONTENTS

List of Tables

List of Figures

Chapter 1. Introduction

1.1 Research Background

The weathered zone is widespread throughout South Korea (Lee, 1993). So, the weathered soil and weathered rock are used as the main foundation layer of various structures due to their high bearing capacity. Therefore, evaluating the ground characteristics of the weathered zone is very important for securing the performance and stability of the structure during design.

However, since it is hard to obtain undisturbed weathered soil samples and weathered rock cores for ground properties evaluation, laboratory tests are difficult to perform and the reliability of the results is low. Therefore, it is common to evaluate the ground characteristics of the weathered zone with field tests such as standard penetration test (SPT), pressuremeter test (PMT), and borehole shear test (BST).

In Figure 1.1, a picture of the typical SPT is shown. The evaluation of the design parameters through the standard penetration test (SPT) uses the SPT-N value and the correlation equation between several parameters (Gang et al., 2018). However, most of the proposals for sand are difficult to apply directly to the weathered zone because its SPT penetration depth is very low compared to that of the sand (Cho et al., 2008).

Figure 1.1 Standard penetration test (SIP eng.)

Figure 1.2 Pressuremeter test apparatus (GS eng.)

A pressuremeter test (PMT) was carried out to evaluate the deformation characteristics of the ground (see Figure 1.2). Pressuremeter, a cylindrical probe with an expandable flexible membrane, is designed to apply uniform pressure to the wall of a borehole (Clarke, 1995). The membrane is expanded against the borehole and the applied pressure and displacement of the membrane are measured simultaneously. The interpretation of the test result and derived parameters are dependent on the ground conditions, the instrument type, the installation method, and the interpretation method. Generally, the pressuremeter test curve can be used to derive in-situ stress state and deformation parameters.

The pressuremeter test can be performed not only in the sand but residual soil and weak rock layers, to determine the ground properties. But there is a limitation that it cannot evaluate the strength properties of the ground, which are the cohesion and the internal friction angle.

Figure 1.3 Borehole shear test apparatus (Handy corp.)

As shown in Figure 1.3, a borehole shear test (BST) was performed to evaluate the strength characteristics of the ground. The BST is a test method for evaluating shear strength by applying horizontal confining pressure to the shear plates which subject to the borehole wall and then pulling it upward.

The determination of internal friction and cohesion are essentially required to solve the stability problems in soil mechanics, including earth pressure, bearing capacity, and slope stability (Luttenegger et al., 1981).

But it is not suitable for testing the weathered zone as the BST apparatus is developed for sand (see Figure 1.3.).

When performing a borehole shear test in a very stiff or overconsolidated soil like weathered zone, penetration of the plates may be prevented, particularly at low normal stresses, and results may be misleading (Hallberg et al., 1983).

1.2 Objective

In this thesis, a borehole pressure-shear test apparatus was newly developed that overcomes the previously mentioned limitations of the existing test methods (SPT, PMT, and BST).

The newly developed test apparatus is suitable for the weathered zone by improving the loading systems and securing the capacity using a motor. Also, it is capable of real-time automatic control and measurement. Moreover, the developed test device can evaluate both the deformation characteristics and strength characteristics of the weathered zone. Since the system for evaluation of strength characteristics is under research and development, the objective of this thesis is to evaluate the deformation characteristics of the ground using the borehole pressure-shear test apparatus. To verify the performance of the test apparatus, a triaxial compression test and a physical model test with developed test apparatus were performed and the results of the experiments were compared.

Via the physical model test result and experimental results by normalization of confining pressure, to review the horizontal loading performance of the developed test device.

Also, the validity of the evaluation of deformation modulus using the developed test apparatus will be reviewed through comparison with the results of the triaxial compression test and physical model test.

1.3 Organization and Structure

This thesis intends to evaluate the deformation modulus and verify the horizontal loading performance using a borehole pressure-shear test apparatus developed based on the theory of pressuremeter test and borehole shear test.

The thesis is structured in the following manner:

A brief literature review on the pressuremeter test based on cavity expansion theory is presented in Chapter 2.

In Chapter 3, the test equipment used in the physical model test was introduced. Then the borehole pressure-shear test apparatus developed for this research is described. As a part of the study, the composition of the newly developed borehole pressure-shear test apparatus, its features, and operation mechanism was delineated. The calibration chamber for physical model tests under controlled laboratory conditions was manufactured. The feature of the calibration chamber for the physical model test was shown. Also, the details (including soil specimen properties and ground conditions) of the physical model tests were described together with the preparation procedure for the model ground in the calibration chamber.

Chapter 4 physical model test results, which were carried out on the model ground, are presented. Via the stress-strain curve obtained from the test results deals with evaluating the deformation modulus of the model ground.

The conclusion and further study are presented in Chapter 5.

Chapter 2. Literature review

2.1 Introduction

A ground investigation is undertaken to determine vertical and horizontal variations in-ground type and ground properties which include the in-situ stress conditions. For example, deformation and strength characteristics of the ground are obtained from investigation results.

There are many techniques used to assess ground conditions and changes in ground conditions ranging from the standard penetration test (SPT) to the borehole shear test (BST). Generally, ground investigation tests can be divided into in-situ tests and laboratory tests which can be further subdivided as shown in Figure 2.1.

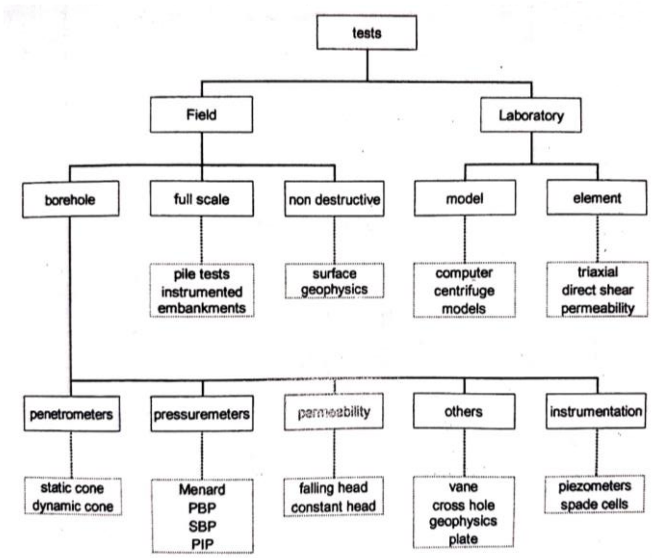

Figure 2.1 Type of in-situ and laboratory tests (Clarke, 1995)

In-situ tests include such as lateral loading test (LLT), pressuremeter test (PMT), cone penetration test (CPT), et cetera. Laboratory tests using sampled or remolded specimens include triaxial test, direct shear test, centrifuge test, et cetera. Usually, when designing, it is difficult to sample undisturbed specimen, so the evaluation of ground characteristics through in-situ tests is mainly performed rather than a laboratory test.

According to Clarke (1995), the only type of in-situ test that can be used in all ground conditions is the pressuremeter. There are different types (Pre-bored, Self-boring, Push-in) of pressuremeter designed for different ground conditions and it is for that reason that this instrument is versatile.

Therefore, in this research, a physical model test similar to the pressuremeter test was performed using a newly developed borehole pressure-shear test apparatus.

In this chapter, the features and background theories of the pressuremeter test and the physical model test using newly developed apparatus were introduced.

2.2 Pressuremeter test

2.2.1 Definition of pressuremeter

The pressuremeter test was developed in France in the early 1950s. Since its development, there has been a considerable growth in the number of designs of pressuremeter that are in use, as will be described below.

Pressuremeter tests can be carried out both in soils and rocks. The pressuremeter probe, which is a cylindrical device designed to apply uniform pressure to the ground via a flexible membrane, is normally installed vertically, thus loading the ground horizontally (see Figure 2.2).

It is connected by tubing or cabling to control and measuring unit at the ground surface. A pressuremeter test aims to obtain information on the stiffness, and in weaker materials on the strength of the ground, by measuring the relationship between radial applied pressure and the resulting deformation (Clayton et al., 1982; Clarke, 1995).

Generally, radial pressure and displacement are monitored during a pressuremeter test and these data are used to produce a stress-strain curve from which parameters or ground properties are determined.

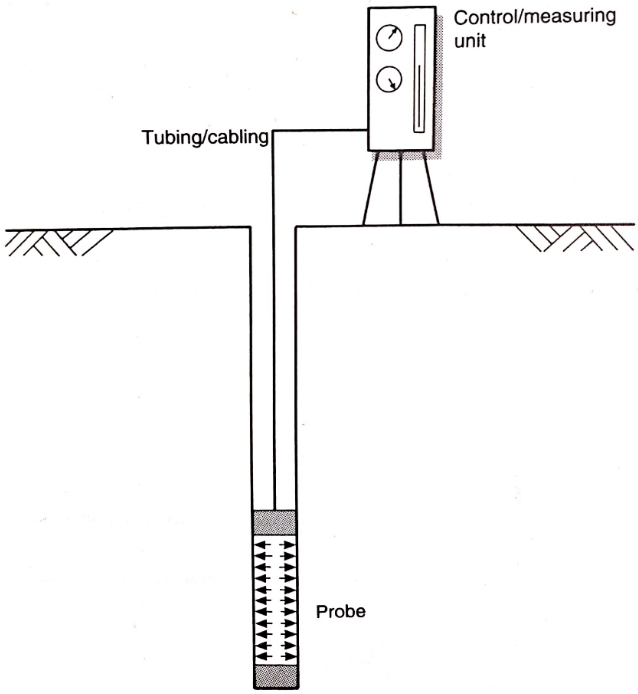

Figure 2.2 Basic components of the pressuremeter (Clayton et al., 1982)

Similar to the pressuremeter in Figure 2.2, the newly developed borehole pressure-shear test apparatus in this research has a configuration of the upper control box and lower probe. This will be covered in detail in Chapter 3.

2.2.2 Features of pressuremeter

As shown in Figure 2.2, the pressuremeter is composed of three parts: the probe, the control unit, and the cabling for the probe and control unit.

The probe has an expanding section, can either be a mono-cell or tri-cell, and may or may not include transducers. It comprises an expanding membrane usually which can be made from natural rubber. Metal membranes are used where small displacements are anticipated and hence are not common. The membrane is supported on sleeves on the body of the probe during installation, and during a test, the membrane is expended by forcing oil, water, or gas into the probe. By measuring the pressure and displacement applied to the membrane, the behavior of the ground can be verified. The test section (expanding section) has a finite length. It is assumed that it expands as a right circular cylinder. Volume displacement type probes usually contain flexible guard cells. These probes are known as tri-cell probes. Radial displacement type probes usually have only one expanding section and are known as mono-cell probes.

The control unit is used to control and monitor a test. In its simplest form, it consists of a pressure supply, which can be either a gas supply or a hydraulic pump, a displacement and pressure measurement unit, and a pressure or displacement control system. Pressuremeter tests can either be stress or strain-controlled, or a combination of stress and strain-controlled. In stress-controlled tests the volume or displacement of the membrane is measured; in strain-controlled tests, the applied pressure is measured.

The types of pressuremeter

There are three groups of pressuremeters depending on the installation system.

Pre-bored type (PBP): This type of pressuremeter is originally developed by Menard (1955). In the original Menard system, the probe contains a measuring cell which is fluid-filled as shown in Figure 2.3.a. The radial expansion of the probe when pressurized is inferred from measurements of volume take made at the ground surface, using the control/measuring unit. A guard cell is incorporated into each end of the probe, to ensure, that the measuring cell expands only radially.

Self-boring type (SBP): The self-boring pressuremeter has been developed in an attempt to reduce the almost inevitable soil disturbance caused by forming a borehole. An SBP has an internal cutting mechanism at its base; the probe is pushed hydraulically from the surface, whilst the cutter is rotated and supplied with flush fluid. The soil cuttings are flushed to the ground surface via the hollow center of the probe, as the pressuremeter advances. (Figure 2.3.b)

Pushed-in type (PIP): Pressuremeters pushed into the soil are known as pushed-in pressuremeters (PIP) and if the soil is completely displaced, they are known as full displacement pressuremeters. A PIP is pushed in from the ground surface or the base of a borehole in the same way as a penetrometer is into the soil. (Figure 2.3.c))

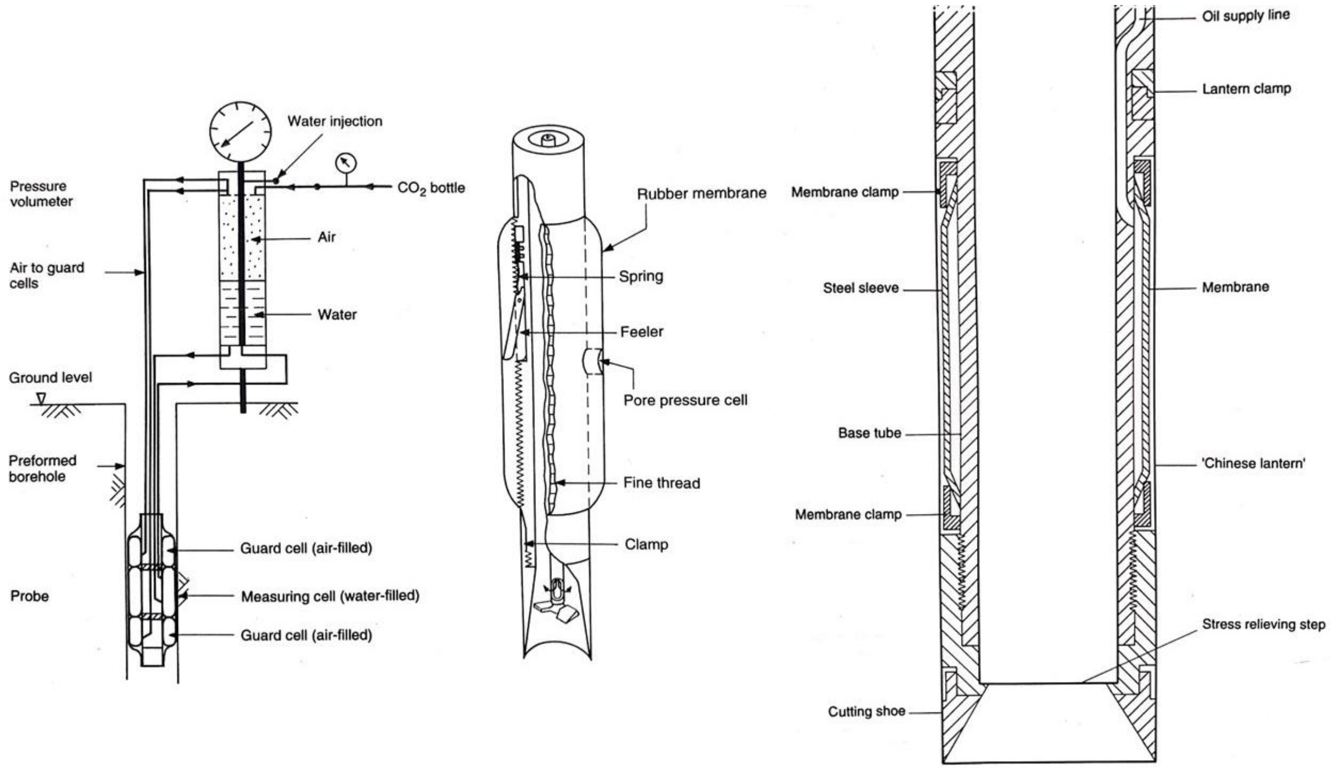

(a)Pre-bored type (PBP) (Gibson and Anderson, 1961)

(b) Self-boring type (SBP) (Windle and Wroth, 1977)

(c) Pushed-in type (PIP) (Henderson et al., 1979)

Figure 2.3 The types of pressuremeter

Generally, the pre-bored pressuremeters can be used in any ground condition, though the sensitivity of the probe must be changed to suit the strength and stiffness of the ground. Self-boring pressuremeters were developed for soil, though they can be used in weak rocks if sufficiently robust. Pushed-in pressuremeters are used in soils.

The borehole pressure-shear test apparatus developed in this study follows the pre-bored type as shown in Figure 2.3.a. The existing pressuremeter uses a flexible membrane for radial expansion, while the newly developed test apparatus was applied rigid shear plates.

Influence factor

Clake (1995) summarized several major reasons for discrepancies between theories of cavity expansion and the practical interpretation of tests. These include:

1) The installation affects the initial size of the cavity and the properties of the surrounding ground.

2) The probe may not be vertical.

3) The vertical stress may not be the intermediate stress once yield has occurred.

4) The horizontal stress may not be the same in all directions.

5) The ground may not behave as a continuum, especially if it contains discontinuities.

6) The ground may not be homogeneous both vertically and radially.

7) Drainage can occur during a test.

8) Ground properties are tested rate dependent.

9) The cavity may not expand as a cylinder.

10) The probe dimensions do not conform to those of a theoretical borehole.

It is for these reasons that simple models are used for the practical interpretation of pressuremeter tests. The pressuremeter tests have been widely used in-situ investigations for design through various interpretation methods of pressuremeter tests by the study of many researchers (Menard, 1957; Gibson and Anderson, 1961; Windle and Wroth, 1977; Houlsby and Withers, 1988; Rerreira and Robertson, 1992; Hughes et al., 1977; Robertson and Hughes, 1986; Luttenegger, 1987; Winter, 1982 and Briaud, 2013). The interpretation of menard pressuremeter, which is frequently cited among them, was applied to this study.

2.3 Interpretation of pressuremeter test

The principal differences between the three classes of pressuremeter described above (Chapter 2.2.2) lie in the stresses applied to the probe at the start of the test. Pre-bored pressuremeters start from a horizontal total stress level close to or equal to zero. Self-boring pressuremeters start their test at approximately the horizontal total stress level in the ground before insertion. A Pushed-in pressuremeter starts with horizontal total stress which can be expected to be much greater than originally existed in the ground. The increases in horizontal total stress applied during the test itself take soil to failure, although in rock this may not be achievable.

Conventionally, Pre-bored pressuremeter test results are plotted in the form of change in volume as a function of applied pressure, whilst Self-boring pressuremeter results are plotted as applied pressure as a function of cavity strain. In Figure 2.4 results from the three types of tests are contrasted schematically.

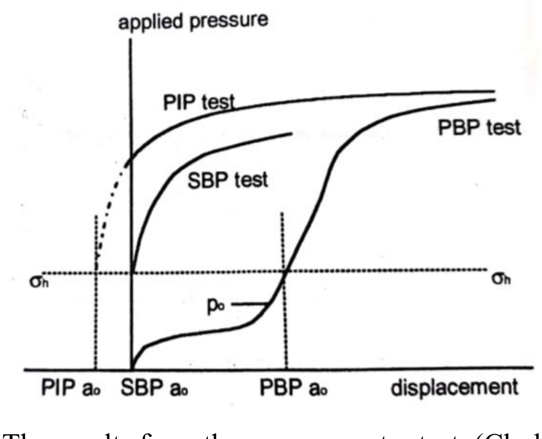

Figure 2.4 The results from the pressuremeter test. (Clarke, 1995)

2.3.1 Analysis of cavity expansion

According to Clarke (1995), an ideal pressuremeter test is often modeled as an expanding cavity in an elastic-plastic continuum. The practical interpretation of a pressuremeter test is more complicated because of the multiphase nature of soils and rocks and the method of installing the probe. Table 2-1, gives references to some of the methods.

Table 2-1 Existing theoretical interpretation of a pressuremeter test.

Researcher	Theoretical interpretation method
Lame (1852)	Linear elastic material
Bishope et al. (1945)	Cohesive material
Menard (1957)	Frictional cohesive material
Gibson and Anderson (1961)	Linear elastic perfectly plastic material with no volume change
Ferreira and Robertson (1992)	Non-linear elastic perfectly plastic material with no volume change
Robertson and Hughes (1986)	Linear elastic perfectly plastic material with volume changes

For the interpretation of the pressuremeter test, consider the ideal situation in which a probe is installed into the ground without disturbing the surrounding material. And the ground is assumed to be homogeneous and isotropic. Lastly, the probe is assumed to be vertical and the length/diameter ratio of the expanding section is large enough such that the pressuremeter test can be modeled as the expansion of an infinitely long right circular cylinder.

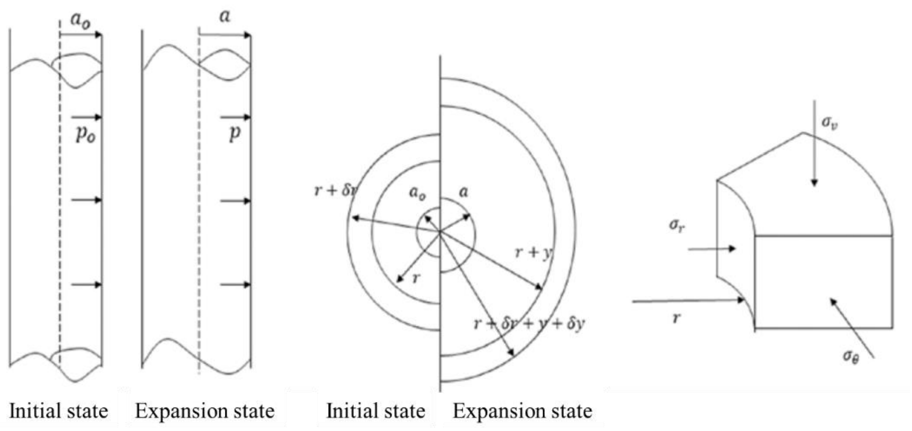

(a) (b) (c)

Figure 2.5 The definitions used in the analysis of the expansion of a cylindrical cavity: (a) expansion of a cylindrical cavity; (b) expansion of an element at radius r; (c) stress on an element at radius r. (Clarke, 1995)

At the start of a test the radius of the probe, or cavity, is a_0 and the internal pressure, p_0, is equal to the total in-situ horizontal stress, σ_h. As p, the applied pressure is increased to p_i the cavity expands in a radial direction to a_i (see Figure 2.5). All movements will be in the radial direction as the length of the cavity is considerably greater than its diameter. Axial symmetry applies as the soil is assumed to be homogeneous and isotropic.

Consider an element of soil, thickness δ_r, at radius r, measured from the center of the cavity, subject to principal stresses σ_r, σ_θ and σ_v. Timoshenko and Goodier (1934) show that the equation of equilibrium is

$$\frac{d\sigma_r}{dr} = -\frac{\sigma_r - \sigma_\theta}{r} \qquad (2.a)$$

The inner radius of the element expands to r + y and the thickness to $\delta r + \delta y$ as the pressure in the membrane is increased from p_0 to p_i. Thus the tensile circumferential strain, ε_θ, is

$$\varepsilon_\theta = \frac{y}{r} \qquad (2.b)$$

Since the circumference increases from $2\pi r$ to $2\pi(r + y)$.

The thickness of the element changes by δy, therefore the radial strain, ε_r, is

$$\varepsilon_r = \frac{\delta y}{\delta r} \qquad (2.c)$$

The only variables measured in a test are the applied pressure, p, and the radius of the membrane, a. The circumferential strain at the cavity wall is referred to as the cavity strain, ε_c, which is defined as

$$\varepsilon_c = \frac{a - a_0}{a_0} \qquad (2.d)$$

There are instances in which the volume of the cavity is measured. The change in volume, ΔV, is simply related to the cavity strain by

$$\frac{\Delta V}{V} = 1 - \frac{1}{(1+\varepsilon_c)^2} \qquad (2.e)$$

Where V is the current volume. It is assumed that at some distance from the probe the strain and the change in radial stress are zero; that is $\sigma_r = \sigma_h = \sigma_\theta$ and $\delta y = 0$.

The test apparatus developed in this study evaluates stress-strain behavior through shear plates each having a curvature of 60 degrees instead of a membrane, but applied Equation 2.e under the assumption that radial expansion.

2.3.2 Pressuremeter modulus

The pressuremeter modulus and limit pressure are specific parameters taken directly from a pressuremeter test. The initial pressure applied to the borehole wall is identified as the point P_o as shown in Figure 2.6, at which the pressure increases linearly with strain.

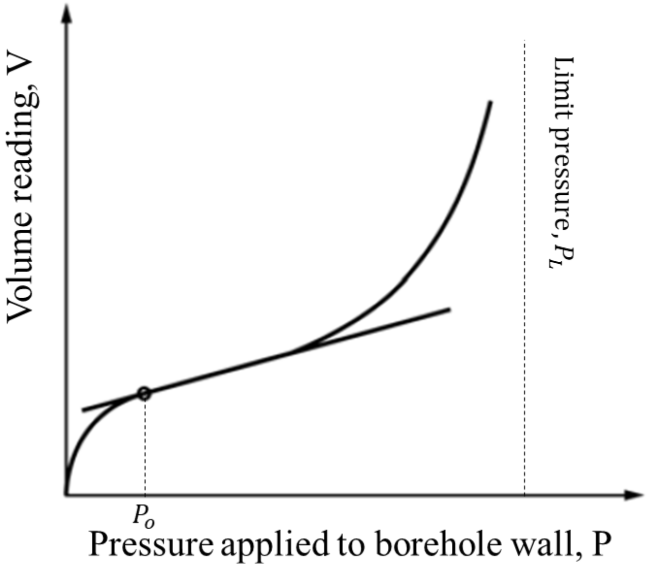

Figure 2.6 Schematic diagram of pressuremeter test results.

The pressuremeter modulus is an elastic modulus taken from the slope which is identified from the curve (Figure 2.6) as the limits of the elastic response. The slope is a function of the shear modulus of the disturbed annulus and gives the pressuremeter modulus, P_m, defined as Equation (2-f).

$$E_m = 2.66[V_o + 0.5(V_B - V_A)]\left(\frac{P_A - P_B}{V_A - V_B}\right) \tag{2.f}$$

Where V_0 is the volume of the probe, V_A is the volume at pressure P_A and V_B is the volume at pressure P_B. The factor 2.66 is based on the assumption that Poisson's ratio for soils is 0.33. The ASTM standard quotes the same formula but permits other values of Poisson's ratio to be used.

The evaluation of deformation modulus using the borehole pressure-shear test apparatus developed in this research is also similar to the general pressuremeter test. As shown in Figure 2.7, an initial elastic modulus is taken from the slope which is identified from the curve. The deformation modulus (initial elastic modulus) was evaluated at a strain rate of 3% from the start of the pseudo-elastic zone.

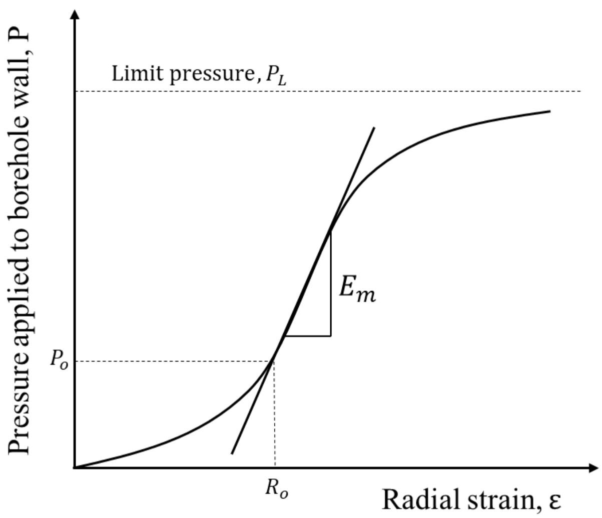

Figure 2.7 Schematic diagram of physical model test results in this study.

2.3.3 Limit pressure

The limit pressure, P_L, is not a fundamental property of soil but is used in design to determine other parameters from the test curve and to compare results from different tests. Limit pressure is defined as the maximum pressure reached in a pressuremeter test at which the cavity will continue to expand indefinitely.

The limit pressure is used to obtain other parameters from correlations with limit pressure (for example, undrained strength, friction angle, or shear modulus) and represent the stiffness response of the ground.

In practice, it is not possible to reach this pressure since the expansion of the membrane is limited. The limit pressure can be obtained by extrapolating the test curve to infinity. According to Menard (1957), the limit pressure is defined as the pressure required to double the cavity diameter.

Similar to the expansion limit of the membrane, the newly developed borehole pressure-shear test apparatus cannot expand the shear plates infinitely. Therefore, the hyperbolic method (Kondner and Zelasko, 1963) was applied to determine limit pressure.

Hyperbolic method

The hyperbolic method was applied to find ultimate stress, $(\sigma_1 - \sigma_3)_{ult}$ by approximating the stress-strain relationship with a hyperbolic, transforming the stress-strain relationship through replotting the stress-strain data as shown below.

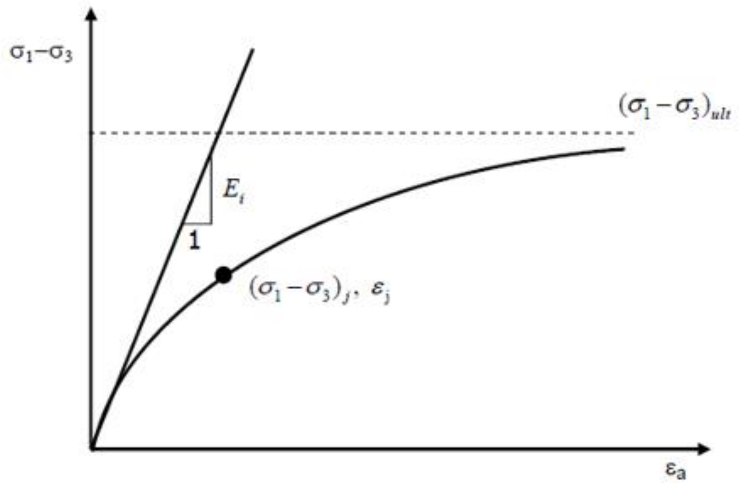

Figure 2.8 Schematic diagram of stress-strain relationship which is approximated by a hyperbola.

Where E_i and $(\sigma_1 - \sigma_3)$ are the initial pressuremeter modulus and effective stress and ε is the strain. The Equation (2.g) can be obtained from any point j in the hyperbola form stress-strain relationship.

$$(\sigma_1 - \sigma_3)_j = \varepsilon_j / \left\{\frac{1}{E_i} + \frac{\varepsilon_j}{(\sigma_1 - \sigma_3)_{ult}}\right\} \tag{2.g}$$

Then, replot the stress-strain data in the form of Equation (2.h) and perform regression analysis.

$$\frac{\varepsilon}{(\sigma_1 - \sigma_3)} = \frac{1}{E_i} + \frac{\varepsilon_j}{(\sigma_1 - \sigma_3)_{ult}} \tag{2.h}$$

As shown in Figure 2.9, the slope of the regression results can be evaluated through replot stress-strain data. Since this slope is the reciprocal of ultimate stress, the limit pressure can be determined.

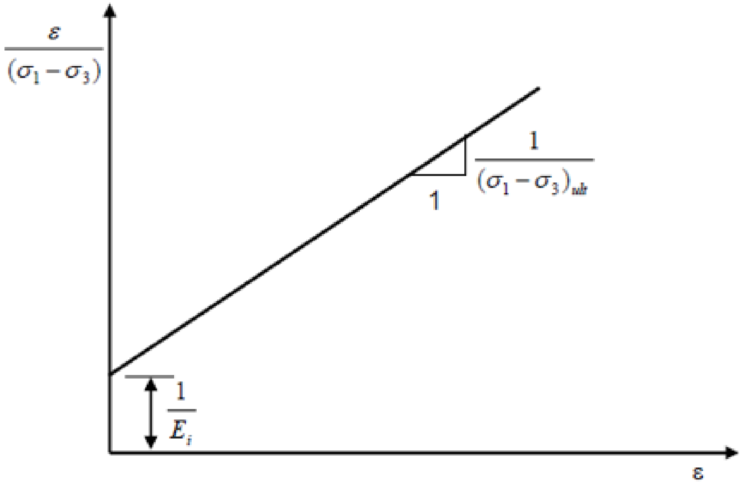

Figure 2.9 Schematic diagram of replot stress-strain data

Chapter 3. Experiment Program

3.1 Introduction

In this chapter, experiment equipment, test material, experiment condition, and experiment procedure, which were adopted in this study are introduced.

The borehole pressure-shear test apparatus developed for this research is firstly described. As a part of the study, the composition of the newly developed borehole pressure-shear test apparatus, its features, and operation mechanism was described.

The calibration chamber for performing physical model tests under controlled laboratory conditions was manufactured. The feature of the calibration chamber for performing the physical model test was shown. A realistic NX-borehole, which has a 76.3mm diameter was physically simulated at the model ground using calibration chamber system and air-pressure loading system, respectively. The test material used was *Yongsan* soil used in Korea. It is uniform weathered soil and classified as SW in USCS. The following conditions relative density, relative compaction, and saturation were determined for the preparation of the sample.

Also, the details (including soil specimen properties and ground conditions) of the physical model tests were described, together with the preparation procedure for the model ground in the calibration chamber.

3.2 Experiment Apparatus

3.2.1 Borehole Pressure-Shear Test Apparatus

The borehole pressure-shear test apparatus is divided into an upper control box and a lower probe, and the detailed configuration is shown in Figure 3.1.

The upper control box is 300mm-width, 300mm-length, 250mm-height, and includes a vertical load cell and motor. The lower probe is a cylinder with a 70mm-diameter and 600mm-height and was developed to perform ground characteristics evaluation in an NX-borehole (diameter, 76mm) in the field. Also, the probe includes a horizontal load cell, a motor, and a wedge element that transmits a vertical force to the shear plates horizontally.

Using this test apparatus, it is possible to evaluate all the deformation characteristics and strength characteristics similar to the PMT and BST results in the field.

In this study, a physical model test was performed using a borehole pressure-shear test apparatus, and the evaluation of deformation modulus was verified by comparing it with the laboratory test, the triaxial compression test.

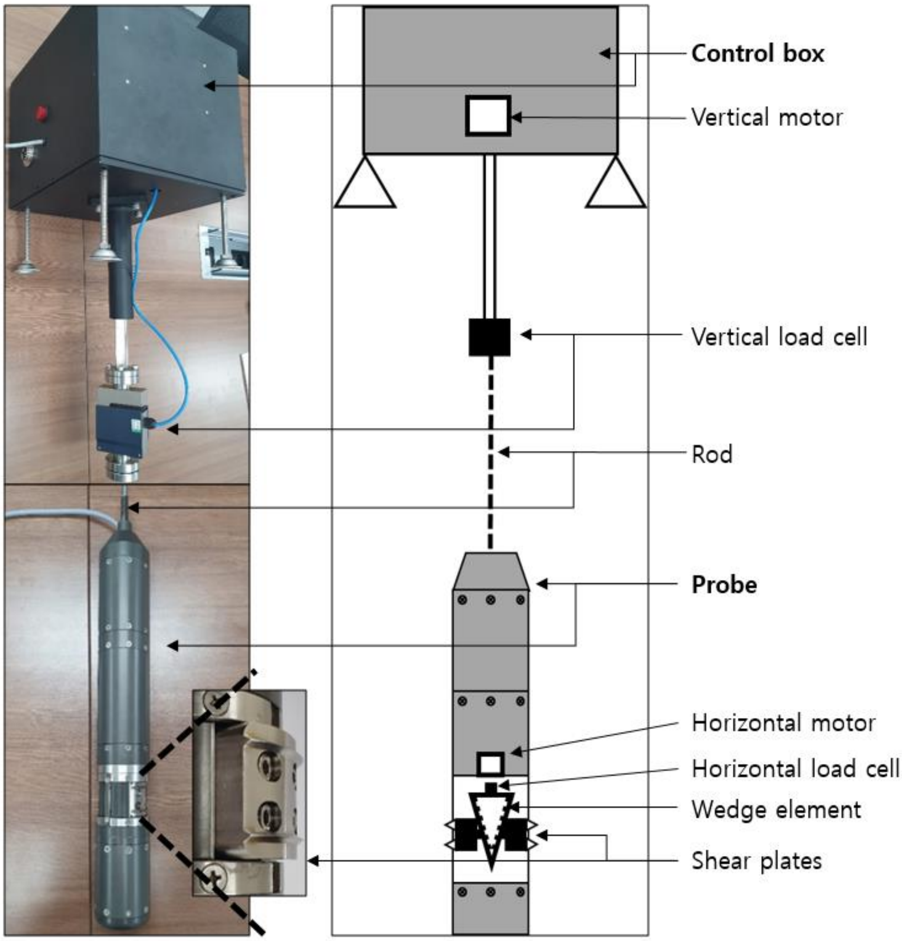

Figure 3.1 Borehole pressure-shear test apparatus (left) and schematic drawing of a Borehole pressure-shear test apparatus (right).

Displacement reading system

In general, the pressuremeter test and borehole shear test are carried out using hydraulic and manual gears. To improve this inconvenience, the newly developed borehole pressure-shear test apparatus used a motor instead of hydraulic and manual gears.

Automatic control and real-time measurement are possible via the motor system so that the ground characteristics of the weathered zone can be easily and conveniently than existing ones. Also, the motor system can secure sufficient capacity and at the same time read the displacement amount without using LVDT (linear variable differential transformer) through the configuration as shown in Figure 3.2. Measurement of displacement without LVDT works as follows.

First, a rotational force is generated by the operation of the horizontal motor. Next, the conchoid connected to the motor rotates together and pushes the nut element down. Lastly, when the wedge member descends together by the nut member, the shear plates fastened to the rail parts of the wedge member moves forward/backward only in the horizontal direction along with the rail parts. So, the displacement deformation can be measured via the encoder according to the number of rotations of the motor.

In the same way, by applying this Encoder-displacement conversion mechanism, the vertical motor in the upper control box can also measure the vertical displacement.

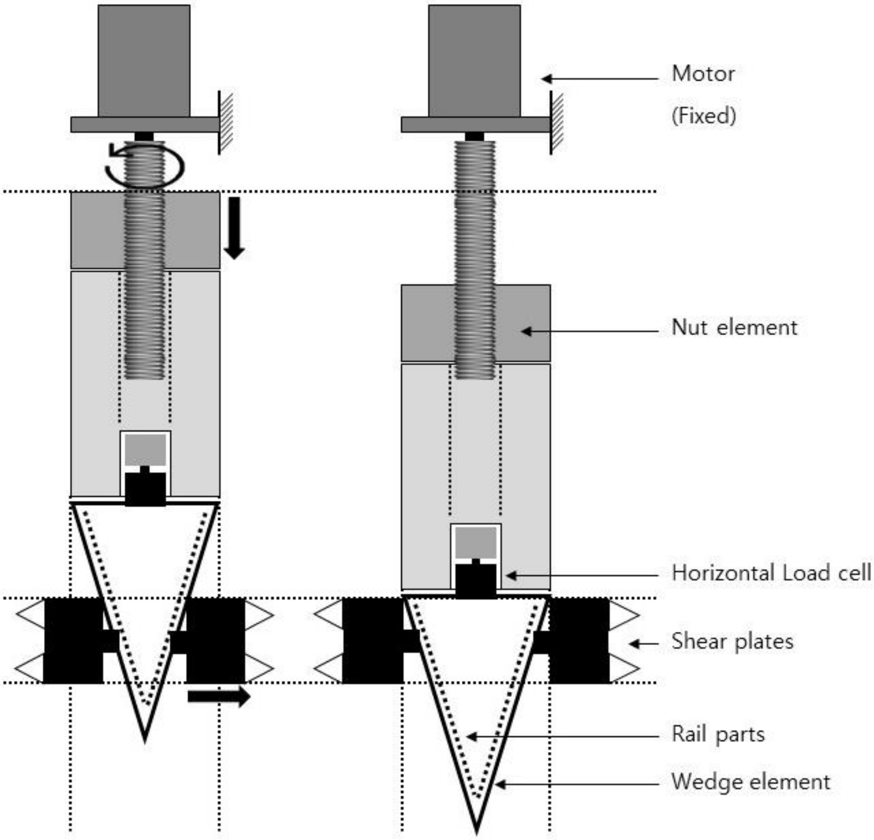

Figure 3.2 Encoder-displacement conversion mechanism of Borehole pressure-share test apparatus.

Horizontal loading system

The horizontal loading system for evaluating the deformation characteristics of the ground works through the lower probe configuration in Figure 3.1.

The rotational force of the horizontal motor is transmitted to the shear plates through the wedge element, and this load can be measured via the horizontal load cell on the wedge element. As illustrated in Figure 3.2, when the wedge element descends, the shear plates move forward, and conversely, when the wedge element goes up, the shear plates move backward. Via this mechanism, as the shear plates penetrate the ground, the load-displacement behavior of the ground can be confirmed.

The loading rate of the shear plates via this horizontal loading system is 0.1%/sec of the constant strain rate. This is sufficiently slower than the loading rate proposed in the existing pressuremeter test method that evaluates the load-displacement behavior. (ASTM-Standards, D4719-07)

Through such a horizontal loading system, it is possible to evaluate the deformation characteristics of the ground using a developed borehole pressure-shear test apparatus.

Specification of the horizontal loading motor is summarized in Table 3-1.

Table 3-1 Specifications of horizontal loading motor

Specification	Horizontal motor
Loading type	Displacement(encoder) control
Maximum loading	5 kN
Loading velocity	0.033 mm/sec
Stroke	0 ~ 15 mm
Motor	IG36PGM
Reduction ratio	1/721

As shown in Figure 3.3, a Sub-miniature load cell, which is a horizontal load cell, and a motor manufactured by CAS were used in this study. The capacity of each measuring device was 10 kN, and 5 kN for the load cell and the motor, respectively. Both measuring devices were connected to the upper control box, and the horizontal load and displacement were stored via the control box at every second.

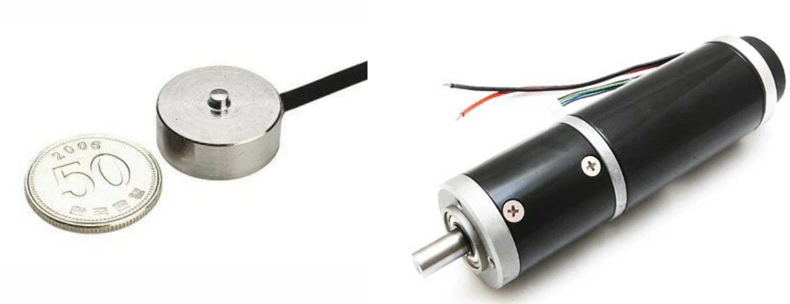

Figure 3.3 Sub-Miniature load cell (left) and Horizontal loading motor (IG36PGM) (right) used in this study.

3.2.2 Calibration Chamber

The physical model test was conducted in a 500-mm-diameter, 500-mm-high three-dimensional laboratory soil chamber. As shown in Figure 3.4, the picture and schematic diagrams of the size of the chamber and soil specimen in this study. The depth of the soil specimen was determined to be 400 mm. in this chapter, the manufacture of the calibration chamber and background theory will be explained.

According to Jang (2008), recently calibration chambers have been used to help in the process of developing correlations between in-situ test results and different soil parameters. The purpose of the calibration chamber test is to evaluate the performance of the various in-situ testing device under strictly controlled laboratory conditions. The most useful advantage of the calibration chamber test is the homogeneous and repeatable sample preparation. Also, the specimen in the calibration chamber has a clear stress history and boundary condition. In a word, through calibration chamber test, homogeneous, repeatable soil specimens subjected to a clear stress history can be prepared and tested under controlled boundary conditions.

To simulate the in-situ test in the calibration chamber, the boundary effect due to the finite boundary should be considered. The factors affecting the boundary effect in the calibration chamber test for sandy soil can be summarized as;

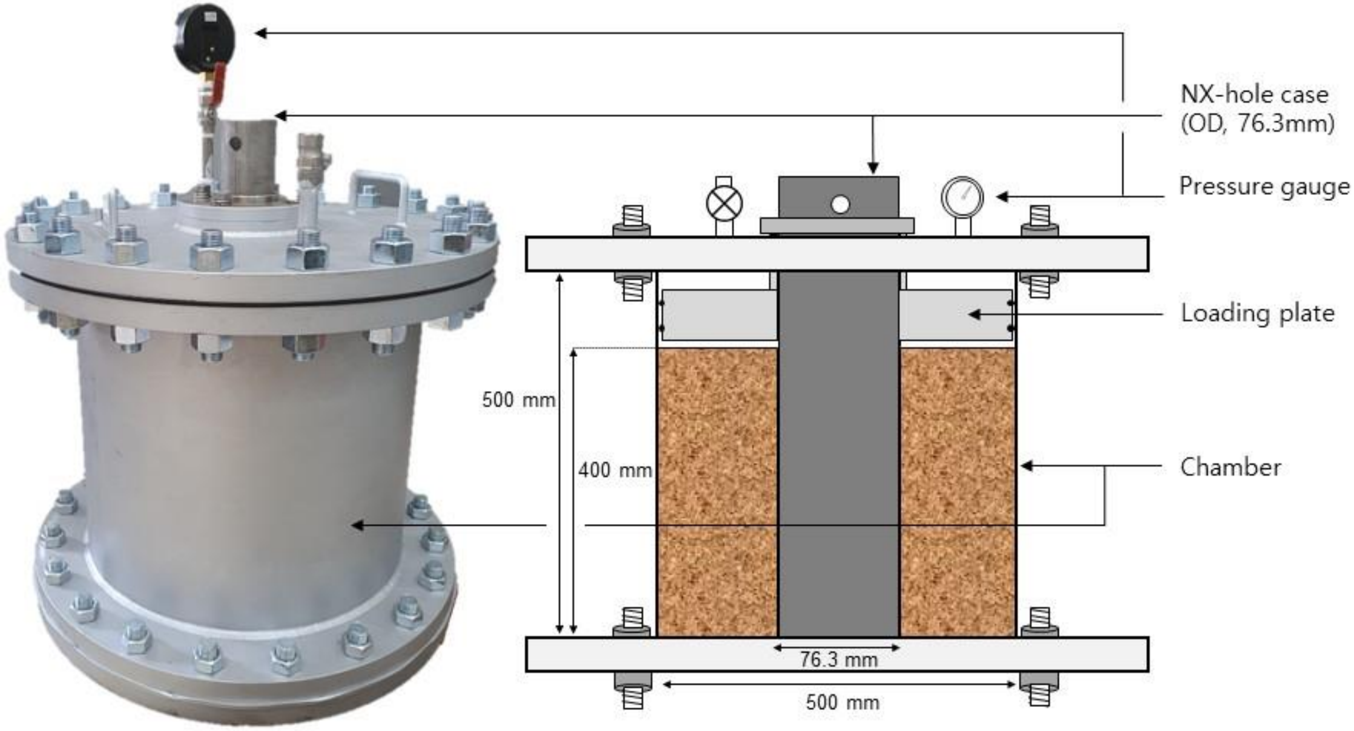

Figure 3.4 Calibration chamber (left) and a schematic drawing of a calibration chamber (right) used in this study.

1) The ratio of the chamber to the diameter of the testing device.

2) The type of boundary (rigid or flexible)

3) The test mechanism

4) Relative density of the specimen

5) Stress states

Most general boundary conditions employed in the calibration chamber are the constant stress condition or no displacement conditions as shown in Figure 3.5. For the flexible wall chamber, it is possible to simulate various stress conditions (BC1). On the other hand, a rigid wall type of calibration chamber can simulate only one-dimensional stress condition (BC2), in which there is no lateral displacement. Also, it is known that the boundary effect of a rigid wall calibration chamber is larger than that of a flexible wall when the size of the lateral boundary is identical.

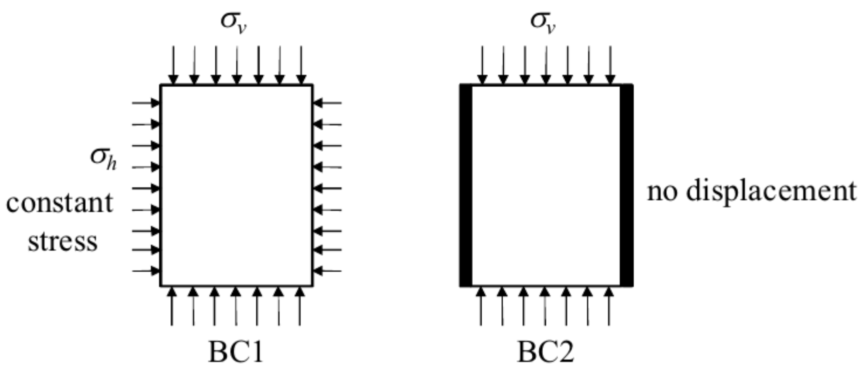

Figure 3.5 Types of general boundary conditions (Jang, 2008)

For the physical model test of this study, the calibration chamber was decided to have a rigid wall. Also, according to the elastic theory (Kai Zhang, 2016), the calibration chamber is large enough to eliminate the boundary effect for studying the response of the borehole, which is 76.3mm in diameter.

Surcharge loading system

The model ground is confined vertically with a rigid loading plate located at the top of the calibration chamber. The surcharge load is applied to the loading plate using the air-compressor line. The surcharge loading system can apply the vertical load up to 500kPa. Through the monitoring of stress using an air pressure gauge, the confining pressure (; vertical load) is measured. (see Figure 3.4)

The surcharge load applied by air pressure is transmitted to the model ground via the loading plate. Because the confining pressure according to the depth can be realized through this surcharge load. In other words, via the calibration chamber and surcharge loading system, field conditions can be simulated in the laboratory.

3.3 Test Material

The test material used in this study is Yongsan residual soil in Korea. It is very uniform weathered soil and is classified as SW in USCS.

Yongsan soil

Particle size distributions of Yongsan soil specimens are presented in Figure 3.6.

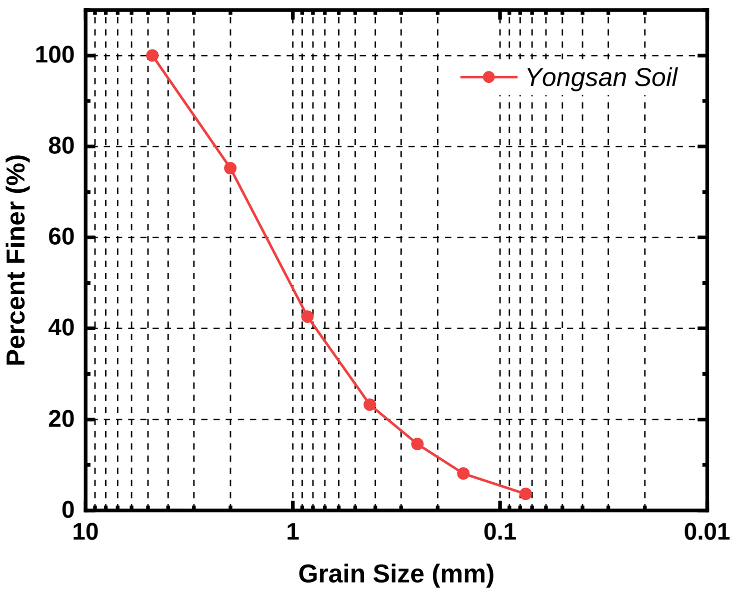

Figure 3.6 Particle size distribution of soil specimens

Yongsan soil, which was sampled near the Yongsan-gu located in Seoul, Korea. Yongsan soil is classified as Well-graded sands (SW) in the Unified Soil Classification System (USCS), 3.59% of which is finer than sieve No. 200, after eliminating a diameter larger than that of sieve No. 4. Also, Yongsan soil was classified as weathered soil, it meets the purpose of this research. The index properties of Yongsan soil are summarized in Table 3-2.

Table 3-2 Index properties of Yongsan soil

USCS classification	SW	Specific gravity, G_s	2.63
Minimum Dry unit Weight, $\gamma_{d\ min}$ (t/m^3)	1.26	Maximum Dry unit Weight, $\gamma_{d\ max}$ (t/m^3)	1.88
Coefficient of Uniformity, C_u	7.9	Coefficient of Curvature, C_c	1.55
Optimum water content, w_{opt} (%)	12.2	Percent finer than # 200 sieve (%)	3.59

The relative density of the model ground of Yongsan soil was predetermined as 55, 77, and 90% which are described as medium, dense, and very dense ground conditions (Das, 1983). The cohesion (c) and internal friction angle (ϕ, ϕ') of each ground condition through the direct shear tests and triaxial compression tests (at 0.5%/hour constant strain rate) were evaluated under the optimum water content condition (w_{opt}).

Direct shear test

For the determination of the consolidated drained shear strength of the soil, the direct shear test was performed. The test method follows ASTM Standards (ASTM, D3080). The shear stress-displacement relationship and vertical displacement-horizontal displacement relationship were obtained via the test results. The results are shown in the following Figures.

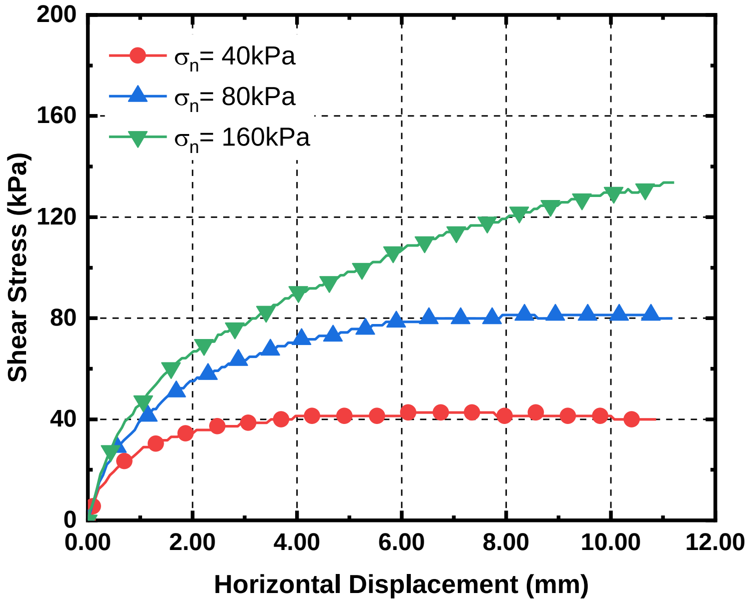

(a) Shear stress-displacement relationships

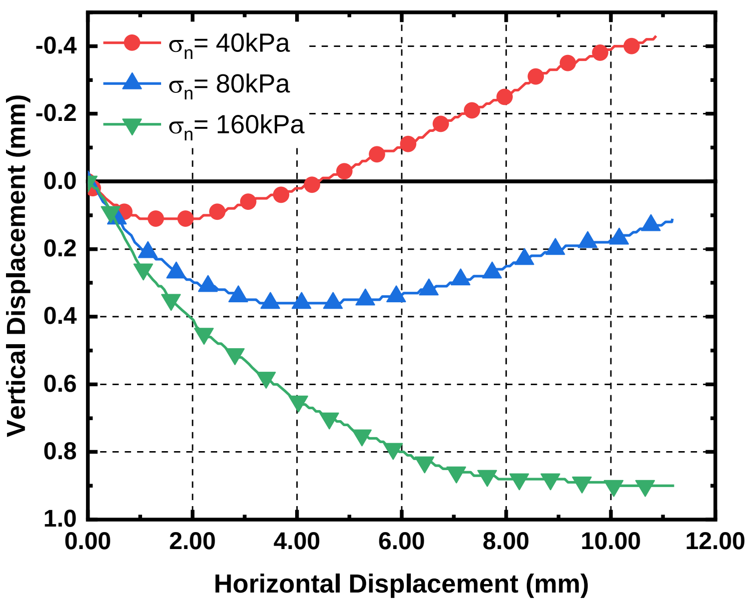

(b) Vertical-horizontal displacement relationships

Figure 3.7 Test results from the direct shear test, D_r = 55%

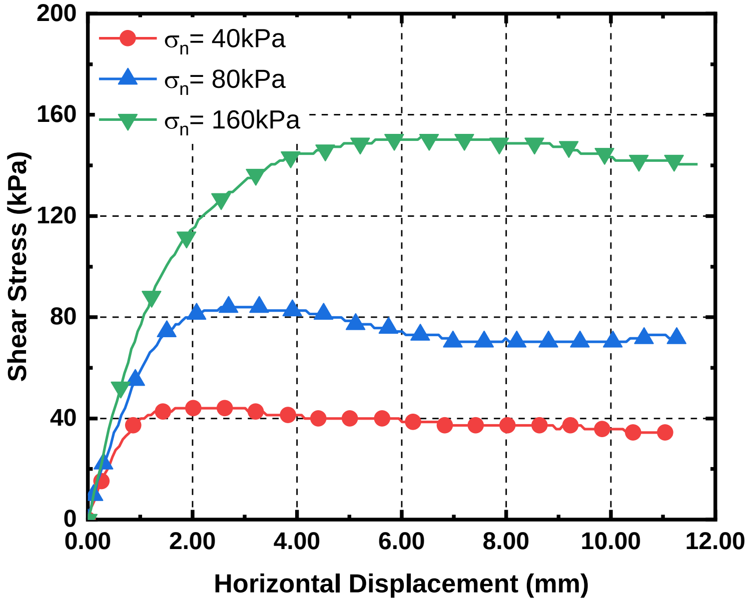

(a) Shear stress-displacement relationships

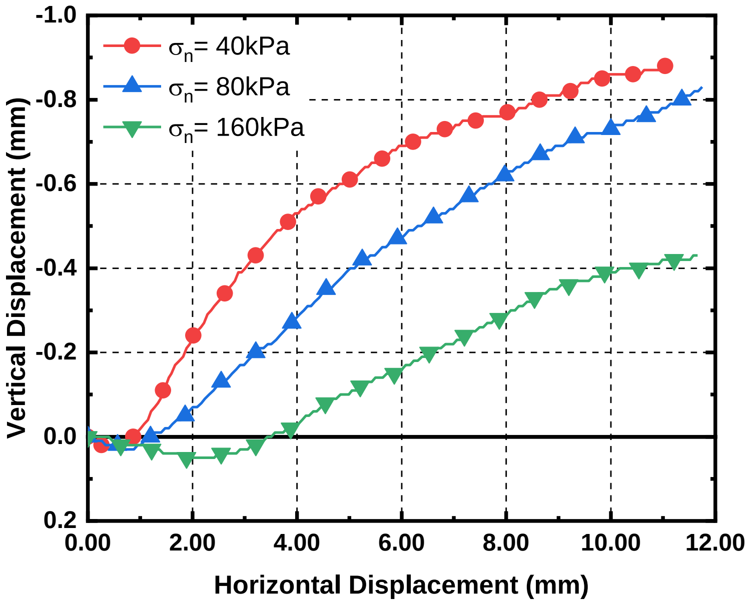

(b) Vertical-horizontal displacement relationships

Figure 3.8 Test results from the direct shear test, D_r = 77%

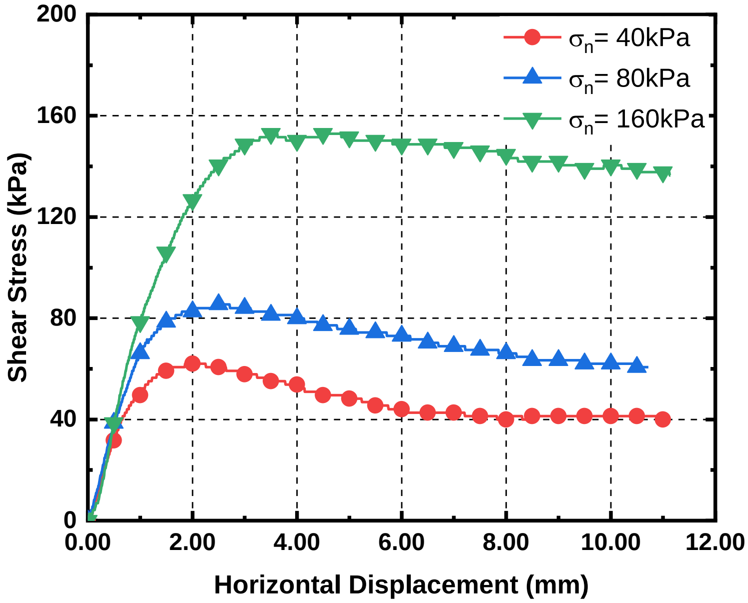

(a) Shear stress-displacement relationships

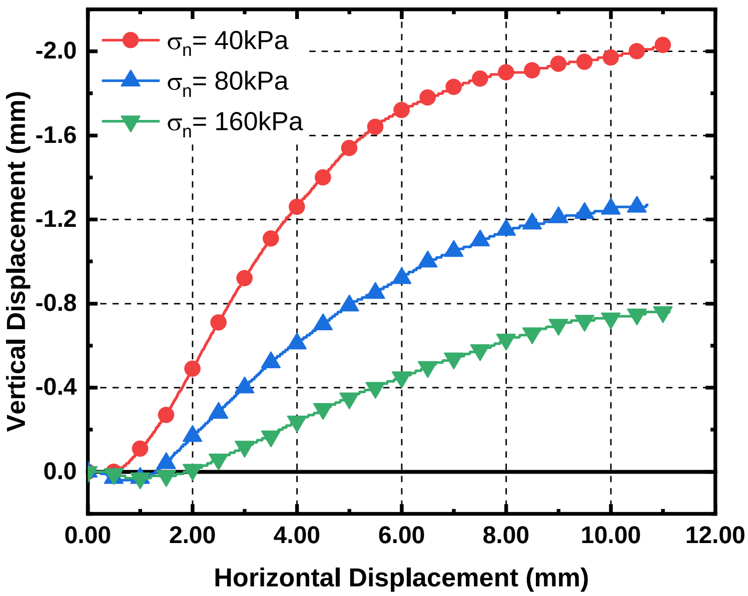

(a) Vertical-horizontal displacement relationships

Figure 3.9 Test results from the direct shear test, $D_r = 90\%$

As shown in Figure 3.10, through the direct shear test, the shear properties of Yongsan soil such as internal friction angle and cohesion were evaluated.

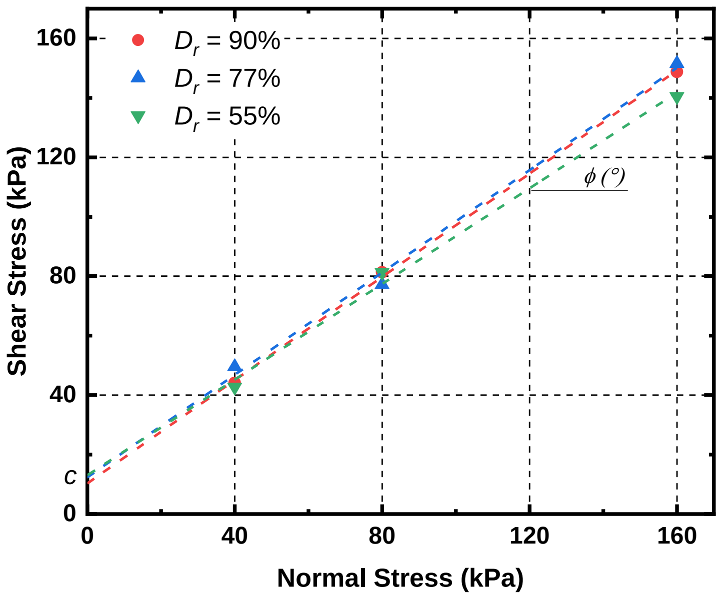

Figure 3.10 Normal stress-shear stress relationships and failure envelop from the direct shear tests

Shear properties of Yongsan soil are summarized in Table 3-3.

Table 3-3 Shear properties of the Yongsan soil

w (%)	D_r (%)	c (kPa)	ϕ (˚)	Description (Das, 1983)
12.2	55	13.09	38.8	Medium state
12.2	77	15.84	40.3	Dense state
12.2	90	10.33	41.0	Very dense state

Triaxial compression test

This laboratory test method covers the determination of strength and stress-strain relationships of a cylindrical specimen of soil. Specimens are consolidated and sheared in compression with drainage at a constant rate of axial deformation (at 0.5%/hour constant strain rate). The test method follows ASTM Standards (ASTM, D7181).

Triaxial compression (CD) test provides data useful in determining the strength and deformation properties such as Mohr-coulomb failure envelops and elastic modulus. Generally, three specimens are tested at different effective consolidation stresses to define a strength envelope. The results are shown in the following Figures.

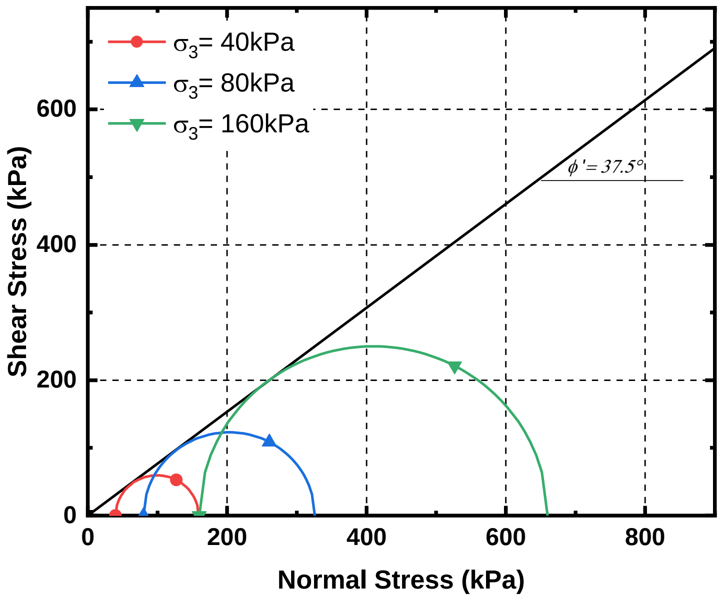

(a) Relative density (D_r) = 55%

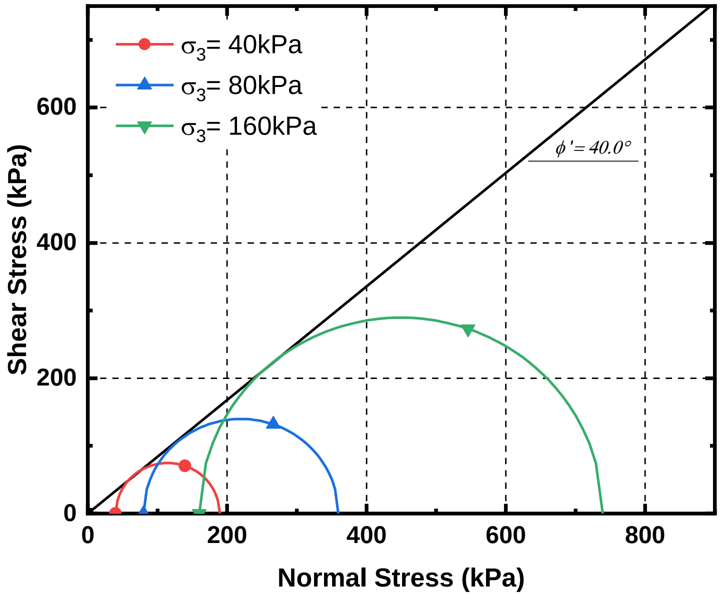

(b) Relative density (D_r) = 77%

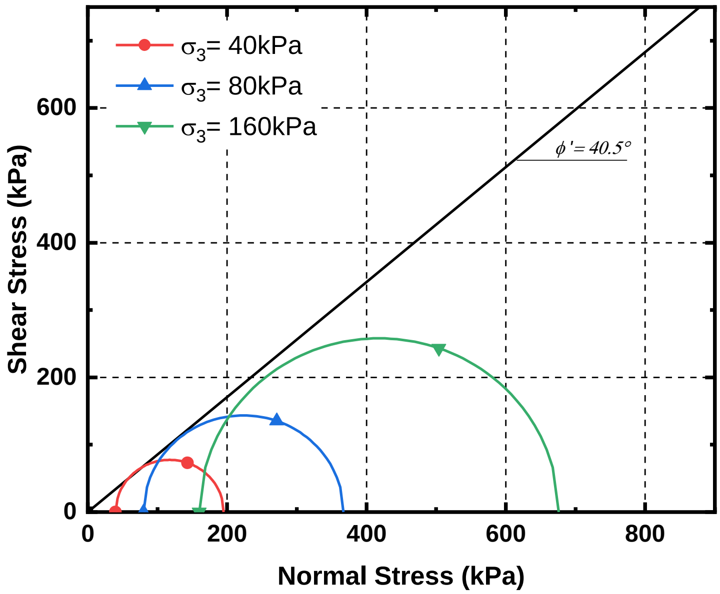

(c) Relative density (D_r) = 90%

Figure 3.11 Mohr-coulomb failure envelop from triaxial compression tests

The shear strength of the Yongsan soil was evaluated through the direct shear tests and the triaxial compression tests were compared and summarized in Table 3-4. As shown in Table 3-4, the shear strength of Yongsan soil according to the ground state (medium, dense, very dense) was similar in both direct shear tests and triaxial compression tests.

Based on the characteristics of the Yongsan soil, the model ground was prepared for the physical model test.

Table 3-4 Shear strength of the Yongsan soil

D_r (%)	DST ϕ (°)	TXC ϕ' (°)	Description (Das, 1983)
55	38.8	37.5	Medium state
77	40.3	40.0	Dense state
90	41.0	40.5	Very Dense state

3.4 Experiment Procedure

3.4.1 Model ground preparation

The Model ground using Yongsan soil was prepared as shown in Figure 3.13. First, combine the NX-hole case as shown in Figure 3.13(a), after that the required amount of dry soil was calculated for the relative densities (55, 77, and 90%) and volume of the calibration chamber. The dry soil specimen was mixed with water to obtain an optimum water content of the soil (12.2%). And then, the prepared moist soil specimen was poured into a calibration chamber, and the consecutive soil layers of a specified thickness (50mm, 8 layers) were compacted with a tamping rammer. The tamping rammer is shown in Figure 3.12.

Figure 3.12 Tamping rammer used in this research

Then assemble the loading plate into the calibration chamber as shown in Figure 3.13(b). In this procedure, if an impact is applied to the NX-hole case, it is easy to disturb the model ground, so pay attention to the assembly.

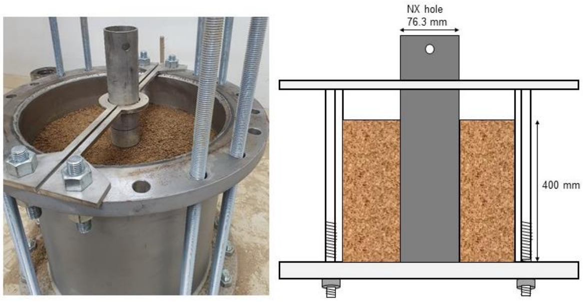

(a) Combined NX-hole case and model ground compaction

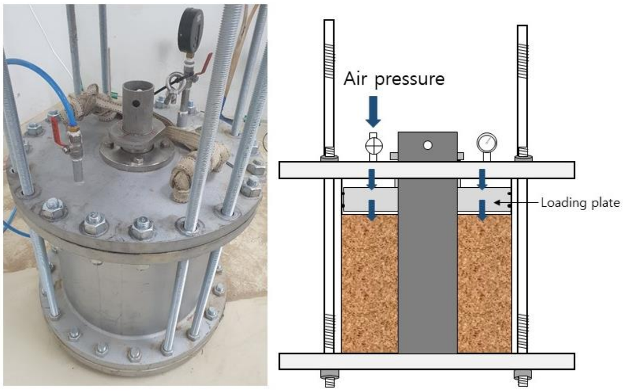

(b) Assemble the Loading plate and Vertical stress loading (air pressure)

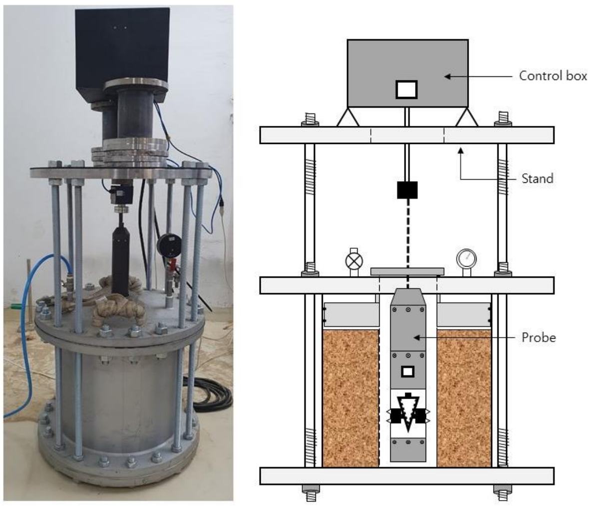

(c) Remove the NX-hole case and Test apparatus setup

Figure 3.13 Preparation of Model ground

After assembly is completed, the surcharge load is loaded via the air-compressor line. The surcharge load is applied by air pressure, and the pressure is not leaked through the calibration chamber and can be adjusted to high pressure (Capacity, 500kPa). After applying the surcharge load, settlement occurs in the model ground. This settlement is measured by LVDT (linear variable differential transformer) to determine the degree of a settlement of the model ground. Then proceed to the next step.

As illustrated in Figure 3.13(c), remove the NX-hole case to perform the physical model test. And a stand that will endure the ground reaction force on top of the calibration chamber is combined. Finally, the borehole pressure-shear test apparatus be set up in the calibration chamber to carry out the physical model test.

Before and after the physical model tests, the relative density and soil water content were measured at several points of the model ground to check the consistency of the model ground.

The model ground conditions using Yongsan soil are summarized in Table 3-5.

Table 3-5 Summary of model ground conditions

D_r (%)	Description (Das, 1983)	w_{opt} (%)	Test no.	Target point	Vertical pressure, σ_v (kPa)
55	Medium state	12.2	T1, T4	Top and Bottom	40
			T2, T5	Top and Bottom	80
			T3, T6	Top and Bottom	160
77	Dense state	12.2	T7	Bottom	40
			T8	Middle	80
			T9	Top	160
90	Very dense state	12.2	T10	Bottom	40
			T11	Middle	80
			T12	Top	160

3.4.2 Physical model test

In this study, a physical model test was performed to verify the evaluation of the deformation characteristics of the ground using a newly developed borehole pressure-shear test apparatus. The evaluation of the ground properties using this test apparatus can evaluate both the deformation characteristics and strength characteristics, but this study deals only with the evaluation of deformation characteristics of the ground.

The procedure of the physical model test is summarized as follows:

1) The model ground was prepared with the pre-determined ground conditions (relative densities, 55%, 77%, and 90%) in the calibration chamber according to Chapter 3.4.1

2) Check the settlement of the model ground by applying a surcharge load, then remove the NX-hole case and set the borehole pressure-shear test apparatus.

3) A horizontal load (0.1%/s of constant strain rate) was applied with the shear plates (see Figure 3.14 right) by horizontal motor power (according to Chapter 3.2.1).

4) The load-displacement behavior can be obtained through the horizontal displacement of the shear plates.

5) The deformation characteristics of the model ground can be evaluated via the results of the horizontal load-displacement behavior.

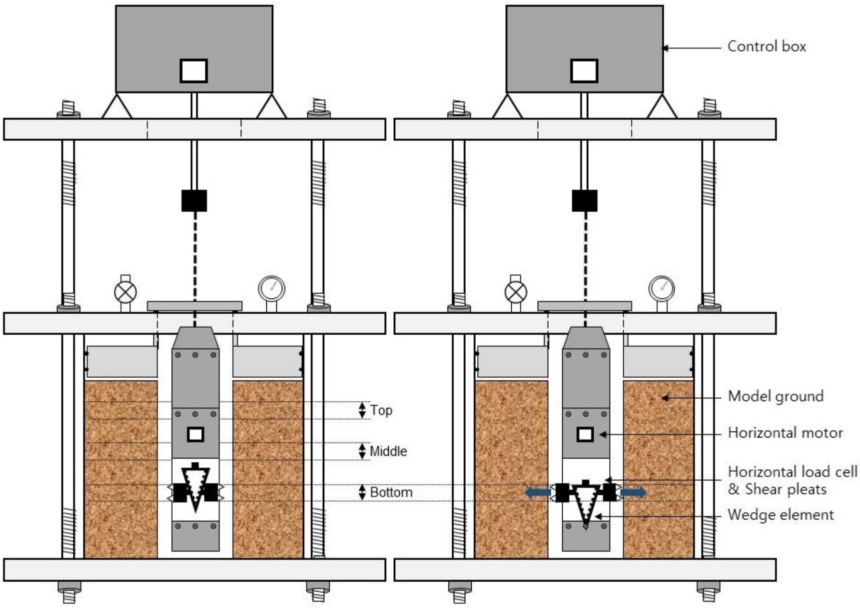

Figure 3.14 Schematic diagram of the physical model test, before the test (left), after the test (right)

After preparing the model ground in the calibration chamber, the borehole pressure-shear test apparatus was placed on the calibration chamber, and check the target point (top, middle, and bottom, see Figure 3.14 left). Subsequently, a horizontal load was applied to the model ground at a constant strain rate of 0.1%/sec, as illustrated in Figure 3.14 right. The strain rate herein was sufficiently slower than the proposed loading late in the existing pressuremeter test (ASTM-Standards, D4719).

During the experiments, the horizontal load and displacement were measured every half second via a control box. The control box can measure the load through the load cell signal and the displacement via the encoder value of the motor. The deformation modulus of the model ground can be evaluated through the results of the horizontal load-displacement behavior.

Chapter 4. Experiment Results and Discussion

4.1 Introduction

This chapter covered results and discussion of the physical model test which was performed on the calibration chamber.

Section 2 of this chapter presented the results of the physical model test. First, the physical model test results according to each relative density (55, 77, and 90%), vertical pressure (40, 80, and 160kPa), and the deformation characteristics of the model ground analyzed through stress-strain curve are listed. Then, in the physical model test, check the difference in the vertical pressure results at the same relative density to understand the effect of the vertical pressure. Also, the effect of vertical pressure is eliminated via the normalization of the experimental results to determine whether a physical model test on a calibration chamber is appropriate. Lastly, a method to determine limit pressure from the experimental results was proposed. Limit pressure can be used in design by having correlating with various ground parameters.

In section 3 of this chapter, a discussion section, through the experimental results, the horizontal loading performance of the borehole pressure-shear test apparatus is verified. Also, by comparing the deformation modulus evaluated via the physical model test and the triaxial compression test, it reviewed whether the deformation modulus evaluation using the developed test apparatus is appropriate. There are some differences in soil mechanics between the two tests, such as the loading direction of the confining pressure and the normal pressure. However, in order to evaluate the deformation characteristics of the specimen, a comparison of the two test results was performed.

4.2 Experiment Results

4.2.1 Deformation modulus

In this section, the physical model test results according to the relative density (55, 77, and 90%) and vertical pressure (40, 80, and 160kPa) are summarized. the deformation modulus was evaluated through the experiment results by applying the background theories described in Chapter 2.

Unlike the existing pressuremeter test, in which a flexible membrane expands in a radial direction, the probe of the newly developed borehole pressure-shear test apparatus applies pressure to the ground horizontally via rigid shear plates. To follow the method of interpreting the pressuremeter test result based on the cavity expansion theory, this physical model test assumes that horizontal pressure acts in the radial direction.

According to the hypothetical theory, the interpretation of the physical model test will be explained through examples of representative experiment results as shown in Figure 4.1.

First, the radial pressure-radial strain curve is the result of the wedge of the shear plates starting to contact the borehole. The wedge of the shear plates penetrates the borehole and the pressure begins to read due to the reaction force of the model ground. Then the strain section (0% ~ 6.8% strain) similar to the wedge height (2.6mm; 6.8% strain) of the shear plates which is non-fully contact and disturbed zone as shown in zone A in Figure 4.1 appears. According to Clarke (1995) suggested that, even with a self-boring pressuremeter, the disturbance during installation could exceed 0.5% cavity strain. In general, the self-boring pressuremeter test is designed to have the least disturbance to the surrounding ground when the probe is installed. However, since the distinction between zone A and zone B is clearly shown in this experiment's results, it was assumed that zone A contains the effects of non-fully contact and disturbed.

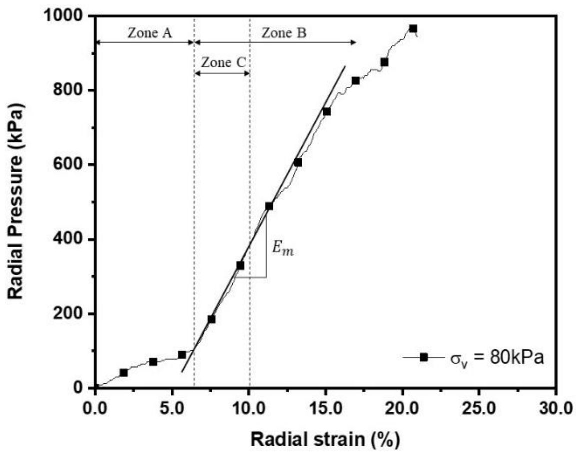

Figure 4.1 Representative example of experiment results

Zone B shown in Figure 4.1 is the pseudo-elastic zone. Zone B, where the slope of the radial pressure-radial strain curve becomes linear, is taken to be the point at which the shear plate fully contacts the surrounding ground. Pseudo-elasticity, sometimes called super-elasticity, is an elastic response to applied stress, caused by a phase transformation of material. In general, this linear section allows an evaluation of the deformation properties of the material.

In this thesis, the deformation modulus of the model ground was evaluated at the strain rate from after zone A to 10% strain. This strain section was used as the analysis zone (;zone C) for deformation modulus determination and is shown in Figure 4.1.

Since this borehole pressure-shear test apparatus is to be applied not only to weathered soil but to weathered rock, the minimum radial strain section applies to all ground conditions was determined. It was noted that the zone C for evaluating the deformation characteristics of the ground was up to 10% strain depending on Clarke (1995). The deformation modulus was evaluated from the slope of zone C, which is the analysis section.

Next, the results of the physical model test performed on the model ground formed with a relative density of 55% are shown in Figure 4.2 below. Also, it is possible to determine the effect of the vertical pressure on the deformation characteristics through the results of applying different vertical pressures.

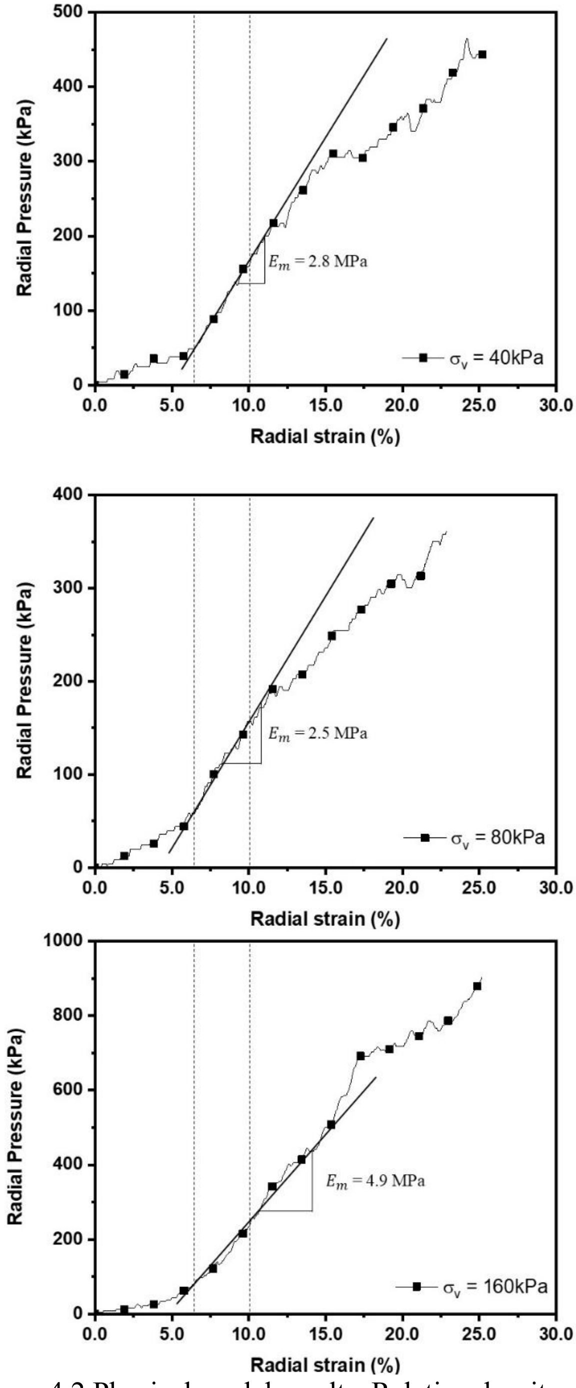

Figure 4.2 Physical model results, Relative density, D_r= 55%

The results of the physical model test in a calibration chamber using the newly developed borehole pressure-shear test apparatus. The physical model test was carried out under the ground condition of 55% relative density, and vertical pressures of 40, 80, and 160kPa were applied to simulate the field conditions, respectively. The deformation modulus via the experimental results was evaluated as 2.8, 2.5, and 4.9 MPa under each vertical pressure condition (40, 80, and 160kPa).

Table 4-1 Comparison of deformation modulus, Relative density, D_r= 55%

Vertical pressure, σ_v	Deformation modulus (MPa)	
	Physical model test, E_m	Triaxial compression test E_{50}
40 kPa	2.8	2.0
80 kPa	2.5	3.3
160 kPa	4.9	4.3

As shown in Table 4-1, deformation modulus through the physical model test and triaxial compression test were compared. The deformation modulus via the triaxial compression test was evaluated based on the laboratory test of Yongsan soil identified in Chapter 3, and E_{50} is the secant modulus in the triaxial compression test results. The comparison of deformation modulus through the two test results showed similar or somewhat higher results evaluated via the physical model test.

From the results that the deformation modulus evaluation performed with the same specimen and the same condition was similar, it can be seen that the deformation modulus evaluation using the developed test apparatus is valid.

And, to confirm the effect of the vertical pressure, the results of physical model tests of 40, 80, and 160kPa are summarized and shown in Figure 4.3.

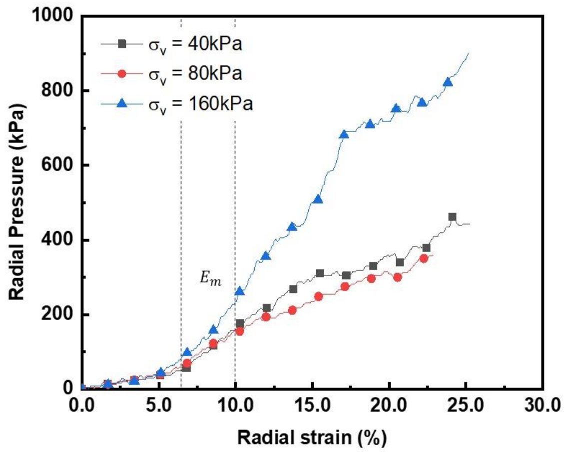

Figure 4.3 Summarized experiment results, Relative density, D_r= 55%

Looking at the summarized experiment results, it can be seen that the radial pressure value tends to increase as the vertical pressure increases to 160kPa. Contrary to this tendency, the vertical pressure 80kPa case shows slightly lower pressure results than the vertical pressure 40kPa case. This is an exceptional case and it is judged to be a result that is difficult to trust. Because of the overlapping effect of the test section due to the wrong selection of target point during the experiment.

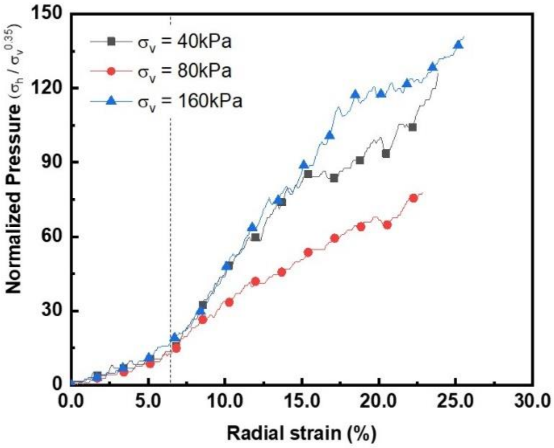

Figure 4.4 Normalized experiment results, Relative density, D_r= 55%

According to Janbu (1964), the deformation characteristics are affected by the vertical pressure, $\sigma_v{}^n$ (n $\approx$ 0.5 for sands, n $\approx$ 0.0 for saturated clays). By applying the theory to the results of this experiment, it was found that $n = 0.35$ of several values fits the physical model test results best.

Through the normalized experiment results, as illustrated in Figure 4.4, it is possible to confirm the tendency that the results of each experiment become similar due to the removal of the effect of the vertical pressure. Also, this analysis shows once again that the reliability of the results of the vertical pressure 80kPa case described above is low.

Next, the results of the physical model test performed on the model ground formed with a relative density of 77% are shown in Figure 4.5 below.

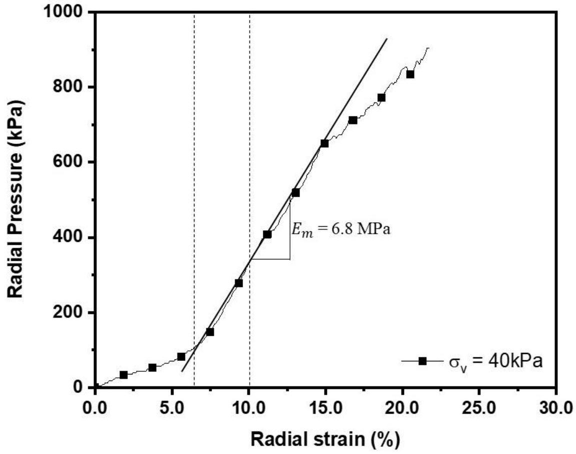

Radial Pressure (kPa)
Radial strain (%)
E_m = 6.8 MPa
σ_v = 40kPa

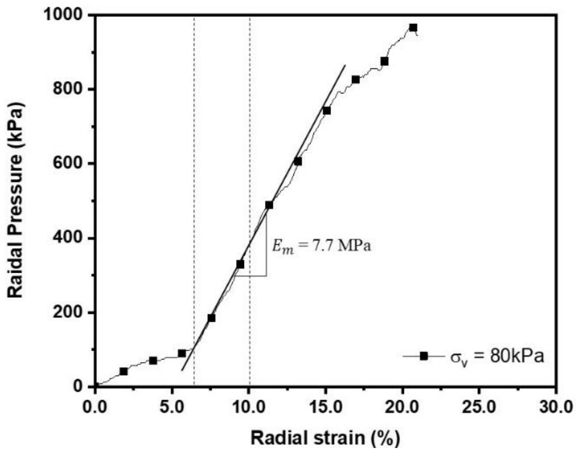

Raidal Pressure (kPa)
Radial strain (%)
E_m = 7.7 MPa
σ_v = 80kPa

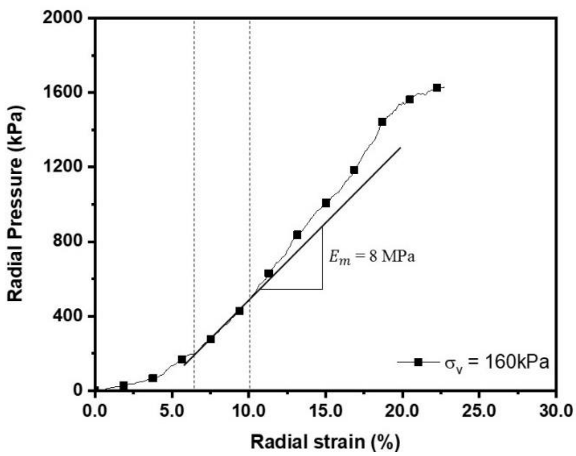

Radial Pressure (kPa)
Radial strain (%)
E_m = 8 MPa
σ_v = 160kPa

Figure 4.5 Physical model results, Relative density, D_r= 77%

The results of the physical model test in a calibration chamber using the newly developed test apparatus. The physical model test was carried out under the ground condition of 77% relative density, and vertical pressures of 40, 80, and 160kPa were applied to simulate the field conditions, respectively. The deformation modulus via the experimental results was evaluated as 6.8, 7.7, and 8.0 MPa under each vertical pressure condition (40, 80, and 160kPa).

Table 4-2 Comparison of deformation modulus, Relative density, D_r= 77%

Vertical pressure, σ_v	Deformation modulus (MPa)	
	Physical model test, E_m	Triaxial compression test E_{50}
40 kPa	6.8	4.3
80 kPa	7.7	6.4
160 kPa	8.0	8.7

As shown in Table 4-2, deformation modulus through the physical model test and triaxial compression test were compared. The deformation modulus via the triaxial compression test was evaluated based on the laboratory test of Yongsan soil and E_{50} is the secant modulus in the triaxial compression test results. The comparison of deformation modulus through the two test results showed similar results evaluated via the physical model test.

From the results that the deformation modulus evaluation performed with the same specimen and the same condition was similar, it can be seen that the ground properties evaluation using the newly developed test apparatus is valid.

And, to confirm the effect of the vertical pressure, the results of physical model tests of 40, 80, and 160kPa are summarized and shown in Figure 4.6.

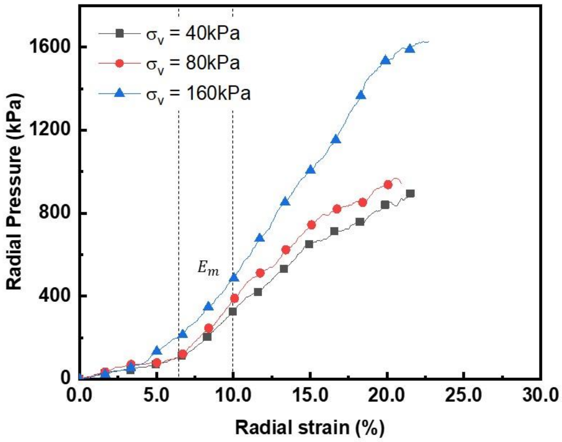

Figure 4.6 Summarized experiment results, Relative density, D_r= 77%

Through the summarized experiment results, it can be seen that the radial pressure value tends to increase as the vertical pressure increases to 40, 80, and 160kPa. This trend shows the effect of the confining pressure as in the general laboratory test results. Based on the ideal results such as summarized experiment results, it was determined that the method of performing the physical model test using the newly developed test apparatus and the evaluation of the deformation modulus of the model ground were appropriate.

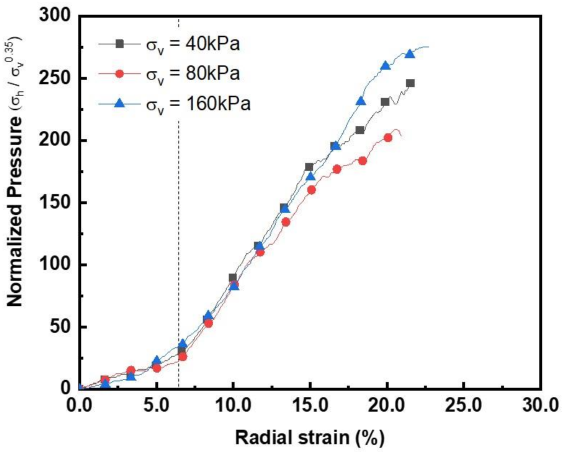

Figure 4.7 Physical model results, Relative density, D_r= 77%

According to Janbu (1964), the deformation characteristics are affected by the vertical pressure, $\sigma_v{}^n$ (n $\approx$ 0.5 for sands, n $\approx$ 0.0 for saturated clays). By applying the theory to the results of this experiment, it was found that $\mathrm{n} = 0.35$ of several values fits the physical model test results best.

Through the normalized experiment results (see Figure 4.7), it is possible to confirm the tendency that the results of each experiment become almost the same due to the removal of the effect of the vertical pressure

Finally, the results of the physical model test performed on the model ground formed with a relative density of 90% are shown in Figure 4.8 below.

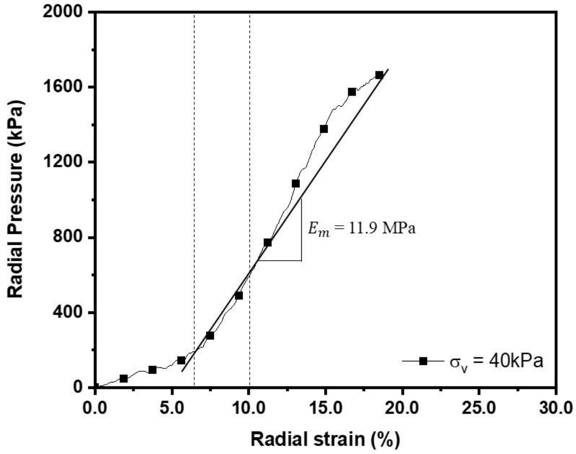
Radial Pressure (kPa)
Radial strain (%)
E_m = 11.9 MPa
σ_v = 40kPa

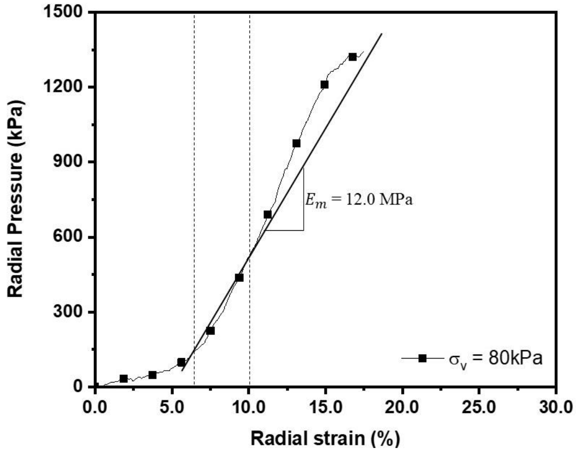
Radial Pressure (kPa)
Radial strain (%)
E_m = 12.0 MPa
σ_v = 80kPa

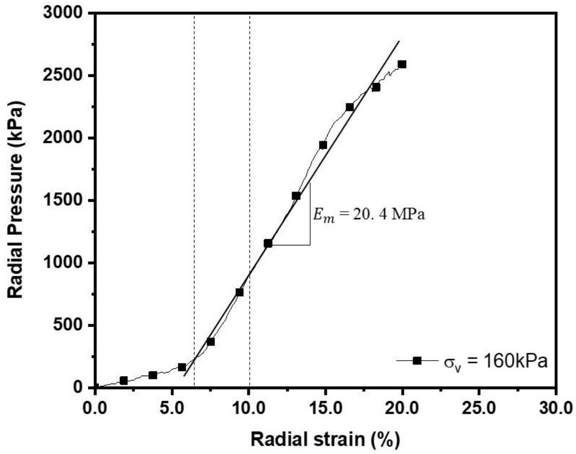
Radial Pressure (kPa)
Radial strain (%)
E_m = 20. 4 MPa
σ_v = 160kPa

Figure 4.8 Physical model results, Relative density, D_r= 90%

The results of the physical model test in a calibration chamber using the developed borehole pressure-shear test apparatus. The physical model test was carried out under the ground condition of 90% relative density, and vertical pressures of 40, 80, and 160kPa were applied to simulate the field conditions, respectively. The deformation modulus through the experimental results was evaluated as 11.9, 12.0, and 20.4 MPa under each vertical pressure condition (40, 80, and 160kPa).

Table 4-3 Comparison of deformation modulus, Relative density, D_r= 90%

Vertical stress, σ_v	Deformation modulus (MPa)	
	Physical model test, E_m	Triaxial compression test E_{50}
40 kPa	11.9	7.15
80 kPa	12.0	10.7
160 kPa	20.4	18.0

As shown in Table 4-3, deformation modulus via the physical model test and triaxial compression test were compared. The deformation modulus through the triaxial compression test was evaluated based on the laboratory test of Yongsan soil, and E_{50} is the secant modulus in the triaxial compression test results. The comparison of deformation modulus via the two test results showed similar or somewhat higher results evaluated through the physical model test.

From the results that the deformation modulus evaluation performed with the same specimen and the same condition was similar, it can be seen that the ground properties evaluation using the newly developed test apparatus is valid.

And, to confirm the effect of the vertical pressure, the results of physical model tests of 40, 80, and 160kPa are summarized and shown in Figure 4.9.

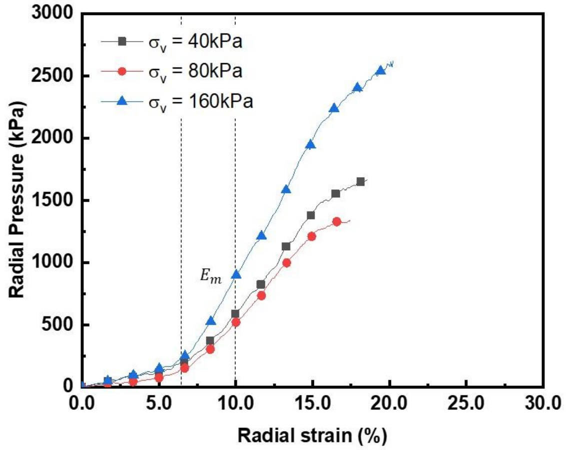

Figure 4.9 Summarized experiment results, Relative density, D_r= 90%

Through the summarized experiment results, it can be seen that the radial pressure value tends to increase as the vertical pressure increases to 160kPa. Contrary to this tendency, the vertical pressure 80kPa case shows slightly lower pressure results than the vertical pressure 40kPa case. This is an exceptional case, and it is judged to be a result that is difficult to trust due to the influence of the disturbance of the model ground when removing an NX-hole case.

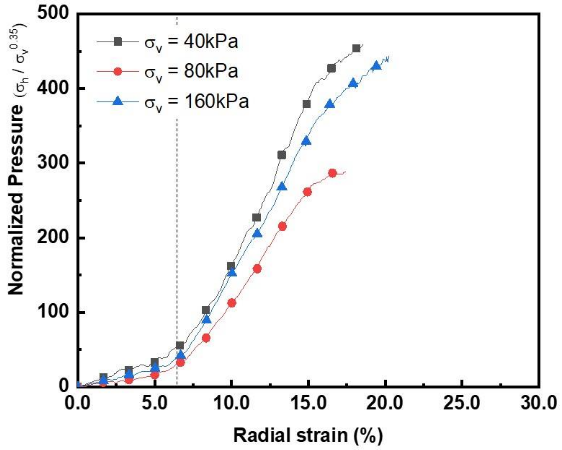

Figure 4.10 Normalized experiment results, Relative density, D_r= 90%

As illustrated in Figure 4.9, the pressure-strain behavior is affected by the vertical pressure, $\sigma_v{}^n$ By applying the theory to the results of this experiment, it was found that $\mathrm{n} = 0.35$ of several values fits the physical model test results best (Janhu, 1964).

Via the normalized experiment results, it is possible to confirm the tendency that the results of each experiment become similar due to the removal of the effect of the vertical pressure. Also, this analysis shows once again that the reliability of the results of the vertical pressure 80kPa case described above is low..

4.2.2 Limit pressure

To determine limit pressure, the hyperbolic method mentioned in Chapter 2 was applied to the experimental results. As shown in Figure 4.11, for evaluation of limit pressure, the hyperbolic method (Kondner and Zelasko, 1963) was applied by dividing it into sections 1 and 2.

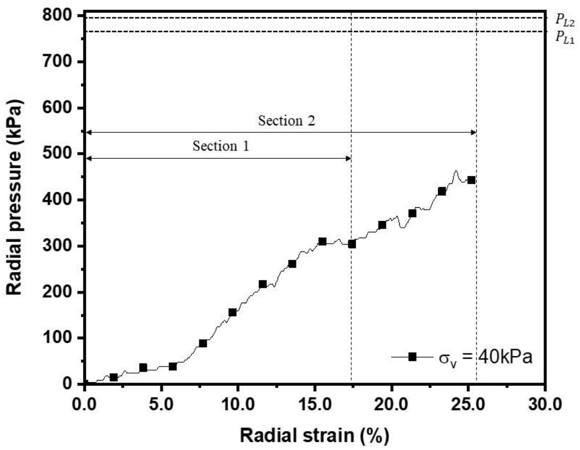

Figure 4.11 Representative examples of limit pressure determination.

As a result of evaluation according to each section, limit pressure (P_{L1}, P_{L2}) was larger than the actual experimental results. This is because the tendency to converge in the pressure-strain curve of the physical model test does not appear clearly. Therefore, to determine and use limit pressure correlated with several ground parameters (σ_h, G, s_u, and ϕ)., it is necessary to apply a method other than the hyperbolic method.

4.3 Discussion

In this section, a discussion section, through the experimental results, the loading performance of the borehole pressure-shear test apparatus is verified. Also, by comparing the pressuremeter modulus evaluated via the physical model test and the triaxial compression test, it reviewed whether the evaluation of deformation modulus using the developed test apparatus is appropriate.

Figure 4.12 summarizes the results of all physical model experiments. As with the aforementioned results, the radial pressure tends to increase as the vertical pressure increases within the same relative density. Likewise, the radial pressure and deformation modulus tend to increase according to the relative density. The deformation modulus of the model ground can be determined through the analysis zone of the radial pressure-strain curve. The evaluation results of the deformation modulus according to each model ground condition are shown in Table 4-4.

Via this, the deformation modulus of the model ground can be evaluated, and the horizontal loading performance of the newly developed test apparatus was verified.

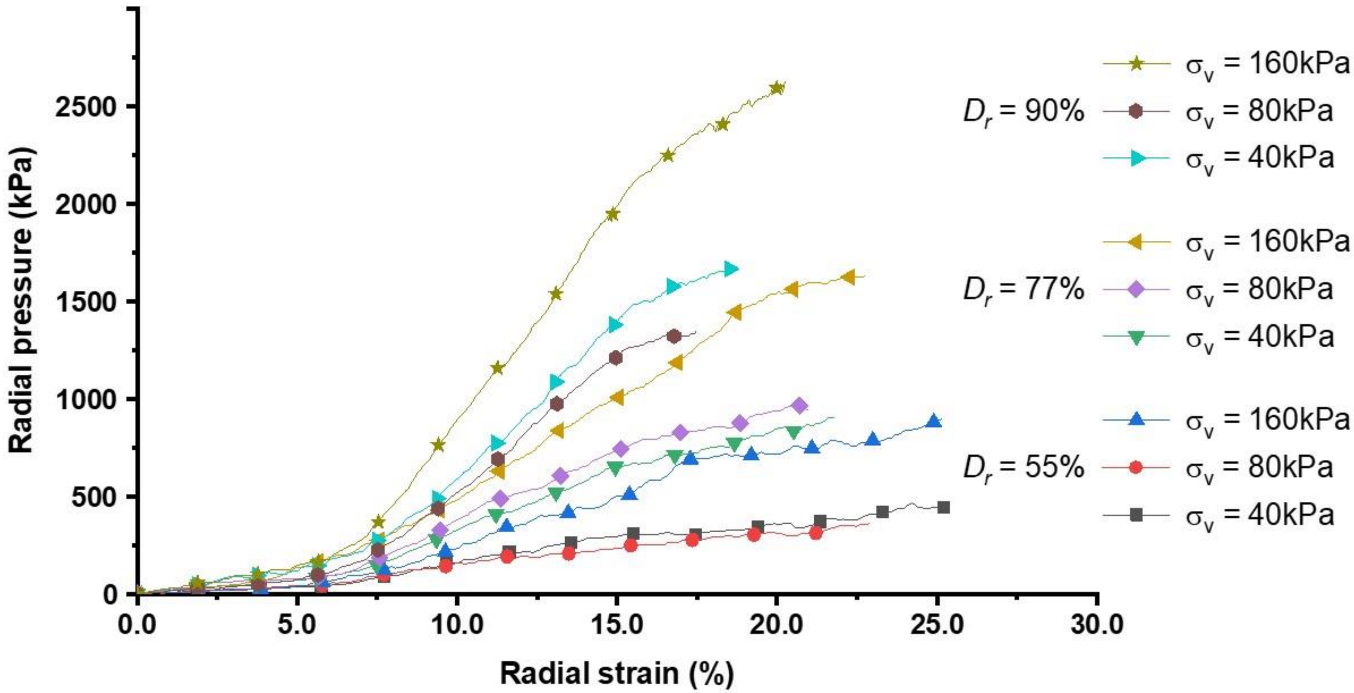

Figure 4.12 Summarizes the results of all physical model tests.

Table 4-4 the evaluation result of the deformation characteristics.

Test conditions		Physical model test	Triaxial compression test
D_r	σ'_v, σ'_3	E_m (MPa)	E_{50} (MPa)
55%	40 kPa	2.8	2.0
	80 kPa	2.5	3.3
	160 kPa	4.9	4.3
77%	40 kPa	6.8	4.3
	80 kPa	7.7	6.4
	160 kPa	8.0	8.7
90%	40 kPa	11.9	7.2
	80 kPa	12.0	10.7
	160 kPa	20.4	18.0

As illustrated in Table 4-4, this is the result of evaluating the deformation modulus of the specimen and model ground according to the relative density and confining pressure. The deformation modulus results from the physical model test and the triaxial compression test appear similar depending on the specimen conditions. The causes of some differences are, it was judged that occurred due to the difference between the strain analysis section and the direction in which the confining pressure applies.

Through this discussion, the validity of evaluating the deformation modulus of the ground using the borehole pressure-shear test apparatus was confirmed.

Table 4-5 the results of deformation modulus compared to secant modulus.

Test conditions		Deformation modulus ratio
D_r	σ'_v, σ'_3 (kPa)	E_m/E_{50}
55%	40	1.400
	80	0.758
	160	1.134
77%	40	1.581
	80	1.203
	160	0.920
90%	40	1.664
	80	1.121
	160	1.133

In Table 4-5, the results of deformation modulus (E_m) compared to secant modulus of elasticity (E_{50}). The deformation modulus ration (E_m/E_{50}) tends to decrease as the confining pressure increases at the same relative density. This result indicates that the physical model test is less affected by the confining pressure than the triaxial compression test. Accordingly, it can be seen that it is appropriate to normalize to $\sigma^{0.35}$ instead of $\sigma^{0.5}$, which is conventionally used in the physical model test normalization mentioned above.

Chapter 5. Conclusion and Further Study

This thesis was conducted to evaluate the deformation modulus and verify the horizontal loading performance using the newly developed borehole pressure-shear test apparatus by physical model tests.

The developed test apparatus can evaluate the deformation characteristics of the ground similar to the pressuremeter test. In this thesis, a physical model test was carried out in a calibration chamber to verify the horizontal loading performance of the developed test apparatus. And then, the deformation modulus of the model ground was evaluated via comparison with the triaxial compression test results.

The conclusions and recommendations drawn from the experiment in this thesis are summarized as follows.

Verification of horizontal loading performance

The experiment results which is pressure-strain behavior of the ground according to the experiment conditions was properly assessed. Also, it was confirmed that the result graphs are similar at the same relative density when the effect of the vertical pressure is excluded from the experimental results through normalization.

These discussions indicate that the surcharge loading system of the calibration chamber was properly applied to the formed model ground. Via this, the horizontal loading performance of the newly developed test apparatus was verified.

The validity of evaluation of deformation modulus

To confirm the validity of evaluating the deformation modulus through physical model tests, the results were compared with that of the triaxial compression test.

Comparing the results of the two tests, it was confirmed that the deformation modulus for both tests was similar at each relative density and confining pressure condition. Through this conclusion, the validity of evaluating the ground deformation characteristics using the borehole pressure-shear test apparatus was confirmed.

Further study

The limit pressure is a function of the in-situ stress and stiffness of the ground (σ_h, G, s_u, and ϕ). It is important to evaluate the limit pressure because it tends to be more consistent than other parameters. it is required to improve the hyperbolic method for the limit pressure proposed in this thesis.

Vertical shear performance verification is required. In this thesis, only the horizontal loading performance was verified, but to evaluate the strength characteristics of the ground, a process of verifying the shear performance of the test apparatus via a calibration chamber test is necessary.

Also, it is essential to verify the developed test apparatus through field tests. The deformation and strength characteristics of the ground should be compared based on the results of the pressuremeter test, borehole shear test, and the newly developed tester. Then, an appropriate theory should be applied to interpret the field borehole pressure-shear test results.

Bibliography

Angelim, R.R., Cunha, R.P., Sales, M.M., 2016. Determining the Elastic Deformation Modulus From a Compacted Earth Embankment Via Laboratory and Menard Pressuremeter Tests. Soils and Rocks 39, 285–300.

ASTM-Standards, 2020. Standard test method for consolidated drained triaxial compression test for soils (D7181-20). ASTM Stand. Guid. 1–12. https://doi.org/10.1520/D7181-11.Copyright

ASTM-Standards, 2017. Standard Test Method for Determining In Situ Modulus of Deformation of Rock Using Diametrically Loaded 76-mm (3-in .) Borehole Jack 1 i, 1–7. https://doi.org/10.1520/D4971-16.2

ASTM-Standards, 2017. Standard Test Method for Prebored Pressuremeter Testing in soils. 1-10

ASTM-Standards, 2003. Standard Test Method for Direct Shear Test of Soils Under Consolidated Drained. Test i, 5–12. https://doi.org/10.1520/D3080

Aubeny, B.C.P., Whittle, A.J., Ladd, C.C., Member, H., 2003. Effects of Disturbance on Undrained Strengths Interpreted from Pressuremeter tests 3, 1133–1144.

Baek, S.H., Shin, G.B., Chung, C.K., 2018. Assessment of the side thrust for off-road tracked vehicles based on the punching shear theory. J. Terramechanics. https://doi.org/10.1016/j.jterra.2018.07.002

Briaud, J.-L., 2013. Ménard Lecture The pressuremeter test: Expanding its use Conférence Ménard L'essai pressiometrique : élargissement de son utilisation. 18th Int. Conf. Soil Mech. Geotech. Eng. 107–126.

Clarke, B.G., 1995. Pressuremeters in geotechnical design. published by Blackie Academic and professional, an imprint of Chapman & Hall.

Clarke, B.G., Carter, J.P., Wroth, C.P., 1979. In situ determination of the consolidation characteristics of saturated clays. Des. parameters Geotech. Eng. Proc. 7th Eur. Conf. soil Mech. Found. Eng. Bright. 1979. Vol. 2, (British Geotech. Soc. Distrib. by T. Telford, London) 207–211.

Clayton, C.R.I. and Matthews, M.C. and Simons, N.E., 1982, Site Investigation, published by Granada Publishing Limited - Technical Books Division, 487-500.

Cunha, R.P. Da, 1994. Interpretation of selfboring pressuremeter tests in sand.

Das, B.M., 1983. Principles of Foundation Engineering. PWS-KENT Publishing Company, Boston, MA.

Day, R.W., Thevanayagam, S., 1999. Effect of Fines and Confining Stress on Undrained Shear Strength of Silty Sands. J. Geotech. Geoenvironmental Eng. 125, 1024–1027. https://doi.org/10.1061/(ASCE)1090-

0241(1999)125:11(1024)
Fawaz, A., Hagechehade, F., Farah, E., 2014. A Study of the Pressuremeter Modulus and Its Comparison to the Elastic Modulus of Soil. Study Civ. Eng. Archit. 3, 7–15.
Gang, B., Hwang, B., Cho, W., Society, K.G., Information, C., 2018. 표준관입시험 N값을 활용한 지반정수의 경험적 산정 Empirical Estimations of Soil Constants Using Standard Penetration Test N Value.
Gangopadhyay, C.R., Nasr, A.N., 1986. Interpretation of Pressuremeter Tests Using Laboratory Simulated Tests. ASTM Spec. Tech. Publ. 214–231. https://doi.org/10.1520/stp19288s
Goodman, R.E., Van, T.K., Heuz, E., 1968. Measurement of rock deformability in boreholes. 10th US Symp. Rock Mech. 523–556.
Haberfield, C.M., Johnston, I.W., 1993. Factors influencing the interpretation of pressuremeter tests in soft rock. Symp. Geotech. Eng. Hard Soils - Soft Rocks.
Heuze, F.E., Amadei, B., 1985. The NX-borehole jack: A lesson in trials and errors. Int. J. Rock Mech. Min. Sci. 22, 105–112. https://doi.org/10.1016/0148-9062(85)92332-0
Huang, A.B., Holtz, R.D., Chameau, J.L., 1991. Laboratory study of pressuremeter tests in clays. J. Geotech. Eng. 117, 1549–1567. https://doi.org/10.1061/(ASCE)0733-9410(1991)117:10(1549)
Huang, A. Bin, Fang, C.K., Liao, J.J., Pan, Y.W., 2002. Development of a multiple-purpose borehole testing device for soft rock. Geotech. Test. J. 25, 227–233. https://doi.org/10.1520/gtj11088j
Hwang, H.-S., Choi, Y.-N., Park, B.-S., Yoo, N.-J., 2016. Comparison of Shear Strength Characteristics of Unsaturated Soil From Triaxial Compression Tests with Direct Shear Tests. J. Korean Geosynth. Soc. 15, 63–69. https://doi.org/10.12814/jkgss.2016.15.4.063
Hyperbolic stress-strain responses: Cohesive soils, 1964. . J. Terramechanics. https://doi.org/10.1016/0022-4898(64)90153-3
Ishikawa, T., Fuku, S., Nakamura, T., Momoya, Y., Tokoro, T., 2016. Influence of Water Content on Shear Behavior of Unsaturated Fouled Ballast. Procedia Eng. 143, 268–275. https://doi.org/10.1016/j.proeng.2016.06.034
Janbu, N., 1964. Settlement calculations based on the tangent modulus concept. Three guest lectures at Moscos State University.
Jang, I.S., Chung, C.K., Kim, M.M., Cho, S.M., 2003. Numerical assessment on the consolidation characteristics of clays from strain holding, self-boring pressuremeter test. Comput. Geotech. 30, 121–140. https://doi.org/10.1016/S0266-352X(02)00031-9
Jang, S.H., The effects of strain rate on the pressuremeter test results in sandy soils, Thesis, Seoul National University.

Jansen, J.W., 2015. Correlating Strength and Stiffness Data of the PENCEL Pressuremeter and Triaxial Compression Tests in Florida Sands.
Kim, S., Kim, J., Kim, Y., Society, K.G., 2014. Comparing Initial Young's Modulus of Plane Strain test and Triaxial test.
Kim, Y.-S., Seo, M.-W., Oh, S.-E., 2012. Cyclic Strength and Deformation Characteristics of Marine Cohesive Soil. J. Korean Soc. Agric. Eng. 54, 159–168. https://doi.org/10.5389/ksae.2012.54.3.159
Lee, J., Yun, T.S., Lee, D., Lee, J., 2013. Assessment of K0 correlation to strength for granular materials. Soils Found. 53, 584–595. https://doi.org/10.1016/j.sandf.2013.06.009
Lee, S.G., 2012. 孔內剪斷試驗을 이용한 岩種別 風化帶의 剪斷强度 特性에 관한 硏究., Thesis, University of Seoul.
Lee, S.G., 1993. Geotechnical Characterization of Weathered Granite Soils in Korea. Korean Geotechnical Soc. 9, 5-7.
Lee, S.J., Hwang, S.B., Lee, S.H., Lee, S.H., Kim, K.J., 2014a. Dynamic Properties for Geomaterials of Railway as Determined by Large-scale Cyclic Triaxial Test. J. Korean Soc. Railw. 17, 43–51. https://doi.org/10.7782/jksr.2014.17.1.43
Lee, S.J., Lee, J.W., Lee, S.H., Sagong, M., 2014b. Evaluation of Resilient Modulus for Reinforced Trackbed using Large Triaxial Tests. J. Korean Soc. Railw. 17, 415–422. https://doi.org/10.7782/jksr.2014.17.6.415
Lutenegger, A.J., Timian, D.A., 1987. Reproducibility of Borehole Shear Test Results in Marine Clay. Geotech. Test. J. 10, 13–18. https://doi.org/10.1520/gtj10133j
Matsuoka, H., Liu, S., Sun, D., Nishikata, U., 2001. Development of a New In-Situ Direct Shear Test. Geotech. Test. J. 24, 92–102. https://doi.org/10.1520/gtj11285j
Menard, L., 1957. An apparatus for measuring the strength of soils in place, Thesis, University of Illinois.
Michalowski, R.L., 2005. Coefficient of Earth Pressure at Rest. J. Geotech. Geoenvironmental Eng. 131, 1429–1433. https://doi.org/10.1061/(ASCE)1090-0241(2005)131:11(1429)
Min, K., Lee, J., Lee, J., Lee, D., Jung, C., 2014. The Evaluation of Bearing Resistance of Underreamed Ground Anchor through Realistic Model Experiments. J. Korean Geoenvironmental Soc. 15, 87–92. https://doi.org/10.14481/jkges.2014.15.9.87
Minwoo, S., Bumjoo, K., Iksoo, H., 2009. 대형 직접전단시험과 대형 삼축압축시험에 의한 조립재료의 전단강도 비교 Comparison of Shear Strength of Coarse Materials Measured in Large Direct Shear and Large Triaxial Shear Tests. J. Korean Geo-Environmental Soc. 10, 25–34.
Murphy, K.D., McCartney, J.S., 2014. Thermal borehole shear device.

Geotech. Test. J. 37. https://doi.org/10.1520/GTJ20140009
Öge, İ.F., 2018. Determination of deformation modulus in a weak rock mass by using Menard pressuremeter. Int. J. Rock Mech. Min. Sci. 112, 238–252. https://doi.org/10.1016/j.ijrmms.2018.10.009
Park, Y.B., Chung, H.S., n.d. A Research for Computation of Bearing Capacity and Settlement of Foundation Considering Scale Effect in Weathered-granite Layer.
PENG, K., JIA, R., 2016. Development of the Borehole Direct Shear Testing Apparatus. DEStech Trans. Environ. Energy Earth Sci. 187–191. https://doi.org/10.12783/dteees/seeie2016/4522
Prapaharan, S., Chameau, J.L., Holtz, R.D., 1989. Effect of strain rate on undrained strength derived from pressuremeter tests. Geotechnique. https://doi.org/10.1680/geot.1989.39.4.615
Purposes, G., 2017. Standard Test Methods for Prebored Pressuremeter Testing in Soils 1 1–10. https://doi.org/10.1520/D4719-07.2
Quental, G.R., Universidade, C., Pernambuco, F. De, Sayão, A., Martins, I.S., Poulos, H.G., Hudson, J.A., Marinos, P., Jamiolkowski, M., Mitchell, J.K., Persson, L., Frank, R., Kanji, M., Boscov, M.E., Caldeira, L., Whittle, A., Bérest, P., Baynes, F., Oliveira, R., Cunha, R., 2014. An International Journal of Geotechnical and Geoenvironmental Engineering Special Issue : In Situ Testing for Ground Characterization. An Int. J. Geotech. Geoenvironmental Eng. Spec. Issue Situ Test. Gr. Charact.
Salgado, R., Mitchell, J.K., Jamiolkowski, M., 1998. CALIBRATION CHAMBER SIZE EFFECTS ON PENETRATION RESISTANCE IN SAND By R . Salgado ; Member, ASCE, J . K . Mitchell / Honorary Member, ASCE, J. Geotech. Geoenvironmental Eng. 124, 878–888.
Schnaid, F., Ortigao, J.A.R., Mántaras, F.M., Cunha, R.P., MacGregor, I., 2000. Analysis of self-boring pressuremeter (SBPM) and Marchetti dilatometer (DMT) tests in granite saprolites. Can. Geotech. J. 37, 796–810. https://doi.org/10.1139/cgj-37-4-796
Sedran, G., Failmezger, R.A., Drevininkas, A., 2013. Relationship Between Menard Em and Young’s E Moduli for Cohesionless Soils. Proc. 18th Int. Conf. Soil Mech. Geotech. Eng. 1–6.
Selig, E., Demartinecourt, J., Bauer, G., 1983. The Modified Borehole Shear Device. Geotech. Test. J. 6, 24. https://doi.org/10.1520/gtj10820j
Selig, E., Winter, E., 1982. Suggested Practice for Pressuremeter Testing in Soils. Geotech. Test. J. 5, 85. https://doi.org/10.1520/gtj10807j
Shi, J., Asimaki, D., 2017. From stiffness to strength: Formulation and validation of a hybrid hyperbolic nonlinear soil model for site-response analyses. Bull. Seismol. Soc. Am. 107, 1336–1355. https://doi.org/10.1785/0120150287
Silva, T.Q., Cândido, E.S., Marques, E.A.G., Minette, E., 2016.

Determination of Em from Ménard pressuremeter tests for gneiss residual soils. Proc. 5th Int. Conf. Geotech. Geophys. Site Characterisation, ISC 2016 1, 809–812.
Wangl, Chainchye E., R.H.B., 1996. DEFORMATION CHARACTERISTICS OF PIEDMONT RESIDUAL SOILS By Chainchye E. Wang 122, 822–830.
Won-Chul, K., Hyun-woo, N., Won-Kyun, C., Society, K.G., Information, C., 2003. A Study on the Immediate Settlement on sand.
Woo, S.I., Kim, J., Chung, C.K., 2018. Permeability test device for soil with automatic water head control. Geotech. Test. J. 41, 218–222. https://doi.org/10.1520/GTJ20170047
Yokoyama, T., Sano, O., Hirata, A., Ogawa, K., Nakayama, Y., Ishida, T., Mizuta, Y., 2014. Development of borehole-jack fracturing technique for in situ stress measurement. Int. J. Rock Mech. Min. Sci. 67, 9–19. https://doi.org/10.1016/j.ijrmms.2013.12.008
Yoo, B.S., 2017. A Case Study on Geotechnical Properties and Weathering Degree of Weathered Granite Rock. 한국지반공학회논문집 33, 127–139. https://doi.org/10.7843/kgs.2017.33.12.127
Kondner, R. L., and J. S. Zelasko (1963). A hyperbolic stress-strain formulation of sands, Proc. 2nd Pan Am. Conf. on Soil Mech. and Found. Engrg., Brazilian Association of Soil Mechanics, Silo Paulo, Brazil, 289–324.
Zhang, K., Hou, R., Gamage, R.P., 2016. A modified NX-borehole jack with flexible loading platens. Eng. Geol. 209, 152–162. https://doi.org/10.1016/j.enggeo.2016.05.020
Zhang, L., 2017. Evaluation of rock mass deformability using empirical methods – A review. Undergr. Sp. 2, 1–15. https://doi.org/10.1016/j.undsp.2017.03.003
Zhang, X., Jiang, Q., Kulatilake, P.H.S.W., Xiong, F., Yao, C., Tang, Z., 2019. Influence of asperity morphology on failure characteristics and shear strength properties of rock joints under direct shear tests. Int. J. Geomech. 19, 1–13. https://doi.org/10.1061/(ASCE)GM.1943-5622.0001347

초 록

풍화대(풍화토 및 풍화암)는 높은 지반지지력으로 인해 국내 여러 구조물의 주 지지층으로 활용된다. 이에 따라 풍화대의 지반 특성을 평가하는 것은 설계 시 구조물의 성능과 안정성 확보를 위해 매우 중요하다. 그러나 풍화대는 지반 특성 평가를 위한 불교란 풍화토 시료 및 풍화암 코어의 채취가 어렵기 때문에 실내시험이 불가능하거나 결과의 신뢰도가 낮다. 따라서 표준관입시험(SPT), 공내재하시험(PMT) 그리고 공내전단시험(BST) 등의 현장시험을 통한 풍화대의 지반 특성 평가가 일반적이다.

표준관입시험을 통한 지반 정수의 평가는 SPT-N값과 여러 정수 사이의 상관관계식을 활용한다. 그러나 토사를 대상으로 제안된 것들이 대부분이며 토사보다 SPT 관입량이 매우 적은 풍화대에 직접 적용하기에 어려움이 따른다. 또한, 공내재하시험은 풍화대의 지반 특성을 평가할 수 있으나 점착력과 내부마찰각인 지반의 강도 특성을 평가할 수 없다는 한계가 있다. 마지막으로 공내전단시험은 토사용으로 개발된 전단시험기를 사용하기 때문에 지반의 강도 특성을 평가할 수 있으나 단단한 풍화대 지반에 적합하지 않다.

이에 본 연구에서는 풍화대의 변형 특성 및 강도 특성을 모두 평가할 수 있는 공내재하-전단시험기를 개발하였다. 개발한 시험기는 실시간 자동 제어 및 계측이 가능하고 전단 플레이트 개선 및 모터를 활용한 가압 용량 확보를 통해 단단한 풍화대 지반에 적합하다. 따라서, 하나의 시험기를 통해 지반의 변형 특성 및 강도 특성을 모두 평가할 수 있으나, 현재 강도 특성 평가를 위한 시험기의 일부 기능은 추가 연구 및 개발 중이다. 따라서, 시험기를 활용한 지반의 변형 특성 평가를 위해 삼축압축시험과 공내재하-전단시험기를 활용한 모형시험을 수행 및 비교하였다.

실내에서 수행한 모형시험 결과, 일반적인 실내시험과 유사하게 모형 풍화토 지반의 상대밀도 및 구속압(상재하중)의 크기가 커질수

록 지반의 변형계수가 증가하는 경향을 보였다. 또한, 실험 결과에서 구속압의 영향을 제거하기 위해 정규화하여 비교한 결과, 각각의 상대밀도에서 응력-변형률 거동이 일치하는 경향을 나타내었다. 그리고 동일한 조건에서 수행한 삼축압축시험과 모형시험을 통해 평가한 변형계수 결과가 유사하게 나타났다. 이에 본 연구에서 개발한 공내재하-전단시험기의 수평 재하 성능과 시험기를 이용한 풍화토의 변형 특성 평가의 타당성을 검증하였다.

마지막으로, 시험기의 전단 성능 평가와 현장 시험을 통한 비교와 같은 추후 연구를 통해 공내재하-전단시험기의 현장 적용성 검토가 수행되어야 한다. 또한 본 연구에서 개발한 시험기는 공내재하시험과 공내전단시험 모두를 하나의 시험기로 수행할 수 있어 현장 적용 시 보다 신속하고 효율적으로 지반 특성을 평가할 수 있을 것이라 기대된다.

주요어: 풍화토, 공내-재하전단시험기, 공내재하시험, 모형시험, 압력토조, 변형계수, 시험기개발, 성능검증

학 번: 2018-27331